ANNUAL REVIEWS

Annual Review of Biochemistry

How Messenger RNA and Nascent Chain Sequences Regulate Translation Elongation

Junhong Choi,[1,2] Rosslyn Grosely,[1] Arjun Prabhakar,[1,3] Christopher P. Lapointe,[1] Jinfan Wang,[1] and Joseph D. Puglisi[1]

[1]Department of Structural Biology, Stanford University School of Medicine, Stanford, California 94305–5126, USA; email: puglisi@stanford.edu, junhongc@stanford.edu, rgrosely@stanford.edu, arjunp91@stanford.edu, cpl1@stanford.edu, jinfanw@stanford.edu

[2]Department of Applied Physics, Stanford University, Stanford, California 94305–4090, USA

[3]Program in Biophysics, Stanford University, Stanford, California 94305, USA

Annu. Rev. Biochem. 2018. 87:421–49

The *Annual Review of Biochemistry* is online at biochem.annualreviews.org

https://doi.org/10.1146/annurev-biochem-060815-014818

Keywords

protein synthesis, ribosome, recoding, translation control, mRNA, nascent-peptide chain

Abstract

Translation elongation is a highly coordinated, multistep, multifactor process that ensures accurate and efficient addition of amino acids to a growing nascent-peptide chain encoded in the sequence of translated messenger RNA (mRNA). Although translation elongation is heavily regulated by external factors, there is clear evidence that mRNA and nascent-peptide sequences control elongation dynamics, determining both the sequence and structure of synthesized proteins. Advances in methods have driven experiments that revealed the basic mechanisms of elongation as well as the mechanisms of regulation by mRNA and nascent-peptide sequences. In this review, we highlight how mRNA and nascent-peptide elements manipulate the translation machinery to alter the dynamics and pathway of elongation.

Contents

1. INTRODUCTION

Translation is the end-point of genetic information transfer, where the nucleotide sequence of the messenger RNA (mRNA) dictates the sequence and structure of the nascent protein. The mechanism of protein synthesis is conserved across the domains of life and is driven by the ribosome, a two-subunit RNA-protein machine. Thus, fundamental insights into how the ribosome and the broader translation machinery function have been and will be crucial for understanding gene expression. During translation, ribosomes assemble at the start site marked by a set of three consecutive nucleotides (a codon), add one amino acid encoded by the next codon (decode), move to the next nonoverlapping codon (translocate), and repeat the decoding and translocation steps until a stop codon reaches the decoding center of the ribosome. Repeats of decoding and translocation events are referred to as the elongation phase of translation, where the nascent peptide is elongated by amino acids to build a functional protein.

Our view of translation elongation has evolved over the past decades. In a simplistic model, decoding and translocation events are metrically repeated to produce a nascent protein faithful to the codon sequence within the mRNA. However, this model insufficiently accounted for

numerous instances where the mRNA sequence fails to predict the sequence of the resulting protein. Studies of these special cases of elongation further revealed that local elongation dynamics are influenced by the surrounding mRNA sequences, which create competing elongation pathways that may alter the definition of individual codons. Redefinitions of codons due to dynamic interactions with neighboring mRNA elements are collectively referred to as recoding (1). Recoding is pervasive throughout the domains of life and is especially enriched in viruses. Thus, the static and deterministic view of elongation must be adjusted to include the statistical and dynamic process of recoding. A dynamic view of translation is poised to integrate recent developments in other relevant fields of biology, such as the emerging field of epitranscriptomics, where mRNA can be chemically modified to alter translation.

An enriched genetic code emerges after accounting for the dynamic nature of translation. Various stretches of nucleotide sequences within the mRNA (mRNA elements) regulate the rhythm of its own translation elongation, which in turn dictate the protein structure and function. mRNA elements may cooperatively interact with the translation machinery and alter protein synthesis in a programmed manner. For example, mRNA structures within the coding region have been implicated in recruiting translation factors to aid alternative decoding or disrupt translocation to enhance recoding phenomena (2, 3). In addition, the nature of the newly synthesized protein (nascent-peptide elements) also affects translation, which adds yet another layer of control (4, 5). Nascent-peptide elements together with the mRNA elements can alter translocation or decoding dynamics during recoding (6, 7). This review provides a framework for how various mRNA and nascent-peptide elements affect the dynamics of protein synthesis.

Our richer view of dynamic translation has been driven by improved biochemical, genetic, structural, biophysical, and computational methods. We first discuss the technological developments that have led to our current model of translation elongation. We then review how known mRNA and nascent-peptide elements perturb the dynamics of translation elongation in both decoding and translocation. Finally, we discuss how mRNA and nascent-peptide elements work cooperatively to define the decoding pathway in specific cases of recoding.

2. CURRENT METHODS FOR STUDYING DYNAMICS OF TRANSLATION ELONGATION

The molecular mechanism of translation elongation involves various dynamic structural rearrangements and their coupled chemical reactions. Over the past 50 years, numerous structural, biophysical, and biochemical tools have been developed to observe these different aspects of translation. A detailed molecular mechanism of the translation elongation cycle has been constructed that integrates data from various methods.

2.1. Structural Methods

Structural methods continue to be fundamental in delineating the molecular basis of translation. X-ray crystallography has provided high-resolution views of translational components, including ribosomes. NMR spectroscopy determines structural dynamics of ribosomal domains (8) and nascent protein chains (9)—and recently whole ribosomes using solid state methods (10–13)—but it is hindered by fundamental limitations in solution for large (>500 kDa) systems. Recent advances in cryo–electron microscopy (cryo-EM) have yielded much excitement in the field of translation by providing high-resolution information about translational intermediates and larger complexes that have been previously inaccessible by other structural methods.

X-ray crystallography exposed the first atomic-resolution structures of the translation complex in various functional states. The high resolution (2–3.5 Å) of ribosomal crystallography arises from

the constructive interference of scattered X-rays generated by a regular ordering of biomolecules within a crystal lattice (14), which creates strong X-ray diffraction patterns. The diffraction patterns are used to derive three-dimensional electron densities and, with molecular modeling, the structures of biomolecules are determined. X-ray crystallography has been used to ascertain dozens of high-resolution structures of both bacterial and eukaryotic translation complexes in various functional states. Techniques for crystallization have advanced to allow ligands such as mRNA, transfer RNA (tRNA), and various translation factors to be stably bound to the ribosome during or after crystallization (14). These structures have revolutionized our understanding of translation and provide a molecular blueprint for subsequent engineering of translational components (14). However, high resolution is achieved by molecular ordering, thus eliminating intrinsic macromolecular heterogeneity. Packing of translational complexes within a crystal lattice may induce nonbiological contacts or prevent crystallization of larger assemblies. X-ray crystallography also proves to be difficult in solving unstable intermediates of biological processes that are too transient to be captured and ordered during crystallization.

Cryo-EM avoids many of the pitfalls of X-ray crystallography: Sample heterogeneity is well tolerated; ribosomes can be prepared in a wide-range of near-physiological conditions prior to imaging; and ribosome complexes, which are embedded in vitreous ice rather than forced into a crystal lattice, retain biological contacts. These factors coupled with recent advances in cryo-EM hardware and software have made cryo-EM a powerful method for ribosome structural studies, achieving a near-atomic resolution of intermediate states of translation (15–17). The ensemble of structures in a sample represents the most populated, stable intermediates along the reaction pathway. Similar to X-ray crystallography, cryo-EM does not provide dynamic information, but different structural classes can be ordered post hoc based on structural similarity (17). Time-resolved cryo-EM techniques that use microfluidic chips and environmental chambers for sample preparation rather than the standard sample preparation, which includes mixing, pipetting onto the grid, and plunge-freezing, can be used to capture subsecond intermediates (18, 19). The combination of cryo-EM with time-resolved methods will be a strong driver of future structural work on translation.

2.2. Bulk Kinetics

The static views of molecular architecture provided by the structural methods require a temporal axis. Bulk kinetics (also referred to as ensemble kinetics) based on stopped-flow or quench-flow approaches allow for the determination of rates of chemical reactions with high (millisecond to second) temporal resolution. In a typical bulk kinetics experimental scheme, two solutions are rapidly mixed for a set short period of time, and a fluorescence signal (stopped-flow) or reaction quenching and product concentration (quench-flow) is measured as a function of time. A reaction must be initiated such that all reactants begin their chemical journey simultaneously. However, during multistep or repetitive processes, a bulk collection of molecules can rapidly desynchronize, obfuscating the presence of intermediate states. The usual detection method for the quench-flow approach involves measuring radio-labeled chemicals such as an amino acid or GTP in the reaction quenched at different time points (20). Unlike many chemical transformations, structural changes may be complex and reversible, requiring real-time measurements not accessible using the quench-flow approach. In the stopped-flow apparatus, conformational changes during a reaction can be measured via fluorescence or light-scattering changes in real time (21). These kinetic measurements can be fit to a reaction mechanism model from which the kinetic parameters for the biochemical reactions can be extrapolated.

Recent advances in the bulk kinetics methods have resolved rate constants and processivity factors for multistep chemical reactions, such as penta-peptide formations (22, 23). Measuring kinetics of multistep reactions requires careful formulation of kinetic models, which involves fitting multiple parameters for each reaction step to limited experimental time points. This has been done either by global fitting of multiple parameters (22) or by deriving necessary kinetic reactions to model the process (23). Tracking changes of elongation kinetics during the translation of multiple codons is a crucial feature in studying different mRNA and nascent-peptide elements during translation, where the kinetic effect may occur over multiple cycles of elongation.

2.3. Single-Molecule Methods

Single-molecule methods probe the dynamics of translation due to their ability to detect and sort structural and compositional heterogeneity and observe multiple parallel pathways. Using relatively simple surface functionalization methods, individual biomolecules can be immobilized on an optically transparent surface for prolonged tracking. The single-molecule method provides a tracking of translation over multiple codons without complications arising from complex kinetic models, which is extremely useful in studying mRNA and nascent-peptide elements. Improvements over the past two decades in camera and dye technologies coupled with advances in image analysis methods have led to the explosion of single-molecule fluorescence microscopy methods, allowing detection of temporal changes in composition and conformation of single biomolecules during translation (24–30). The development of optical and magnetic trapping technologies has enabled direct measurement of forces and mechanical stability of molecular complexes (31). Combining fluorescence and force methods will be powerful for studying translation, but it is still technically challenging (32).

Single-molecule fluorescence methods applied to translation led to the identification of key intrinsic dynamic features of the ribosome and its ligands. To track the composition of translational complexes, fluorophores are covalently attached to tRNAs, translation factors, and ribosomes, through numerous methods (26). Observing conformational changes requires pairs of conjugated fluorophores to be proximally located within a typical dynamic range of 20–80 Å to observe single-molecule Förster resonance energy transfer (smFRET) between the two or more dyes. On the basis of the efficiency of FRET, the distance changes between the dye-labeling sites can be detected. Interpreting single-molecule fluorescence data requires specific care to avoid artifacts arising from the experimental setup, which is outlined well in the Ha group's (33) classic review. A combination of multiple smFRET pairs and direct labeling of translational factors has been used to correlate conformational and compositional changes during translation in real time (34–36).

2.4. Ribosome Profiling

Novel DNA and RNA sequencing-based techniques have revolutionized biological measurement. Ribosome profiling (Ribo-Seq) was specifically developed to study translational activity over the entire transcriptome (37–39). The method utilizes the ability of the ribosome to protect actively translated portions of mRNA from RNase degradation, thereby defining, with nucleotide resolution, the position of the ribosome on that mRNA by sequencing the ribosome-protected segments of mRNA. These data are compared with sequencing data on the entire transcriptome in parallel, to discriminate between transcriptional control effects and observed translational control effects. By using the number of sequencing reads and individual mRNA expression levels as standards, Ribo-Seq exposes global translational dynamics with single-base resolution.

Notably, Ribo-Seq is highly sensitive in detecting unexpected and alternative potential protein products synthesized by translating previously unannotated coding regions. Furthermore, subsets of ribosomes can be purified based on their location within a cell or interaction with another factor, revealing different translational profiles within the same cell (40). However, each step in the sample preparation workflow can introduce experimental biases or artifacts. Antibiotic treatments prior to harvesting can bias against rare codons and lead to artificial accumulation of reads at initiation sites (41). The experimental procedure used to generate the deep-sequencing library can also introduce bias (42). Despite such pitfalls, Ribo-Seq can uncover much about the translational dynamics from the whole organism to the level of specific cell types (43). Such sequencing-based approaches will continue to have a large impact on the analysis of genome-wide biophysics during translation and other processes.

3. GENERAL OVERVIEW OF TRANSLATION

The ribosome spatially and temporally coordinates molecular interactions during translation, which can be organized into the four phases of initiation, elongation, termination, and recycling. During initiation, the small (30S in bacteria, 40S in eukaryotes; referred to as 30S here) and large (50S in bacteria, 60S in eukaryotes; referred to as 50S) ribosomal subunits assemble at the start codon to begin protein synthesis via elongation. Elongation ends when the ribosome reaches a stop codon, whereby a protein factor for termination is recruited to release the synthesized nascent polypeptide from the translation complex. The posttermination complex is then disassembled immediately during recycling. Although the initiation, termination, and recycling phases of translation have been shown to be heavily regulated to control the quality and abundance of nascent proteins synthesized from translation (44–49), this review focuses on presenting kinetic and structural schematics of each elongation cycle, where its regulation may lead to different structures and functions of nascent proteins. We discuss mechanisms of how mRNA and nascent-peptide elements regulate protein synthesis in the context of the schematics presented here.

3.1. Elongation Cycle: Decoding

During each elongation cycle, the conformation and composition of the translational complex evolve temporally through several structures (14, 16) (**Figure 1**). Kinetic parameters for each structural transition are well tuned to provide both processivity and fidelity, which is achieved through proofreading steps that monitor the correct codon-anticodon pairing (50, 51). The elongation cycle begins with decoding, where the cognate tRNA is accommodated into the aminoacyl-acceptor tRNA site (A site) and engages (14, 16, 20, 52, 53) with the peptidyl site (P site) bound tRNA. tRNAs may assume various hybrid conformations within the ribosome during the elongation cycle, such as the A/P state, where the first letter denotes its contact with the 30S, and the second letter denotes its contact with the 50S.

Results from different methods have been essential for understanding the process of initial tRNA selection (**Figure 2**). Bulk kinetics were crucial in constructing early models of decoding (20, 52, 53), which are now supported by observations made using other methods such as cryo-EM (16, 54) and single-molecule fluorescence microscopy (24). Collectively, these studies have revealed that decoding begins when aminoacyl-tRNA (aa-tRNA) samples in the T site of the ribosome (**Figure 1**) as a ternary complex (TC) with a GTP molecule and an elongation factor [elongation factor Tu (EF-Tu) in bacteria and elongation factor 1A (eEF1A) in eukaryotes; referred to as EF-Tu here], which increases the affinity of tRNA to the ribosome (55). The anticodon of the sampling tRNA initially does not base-pair with the A-site presented codon (16, 54), but

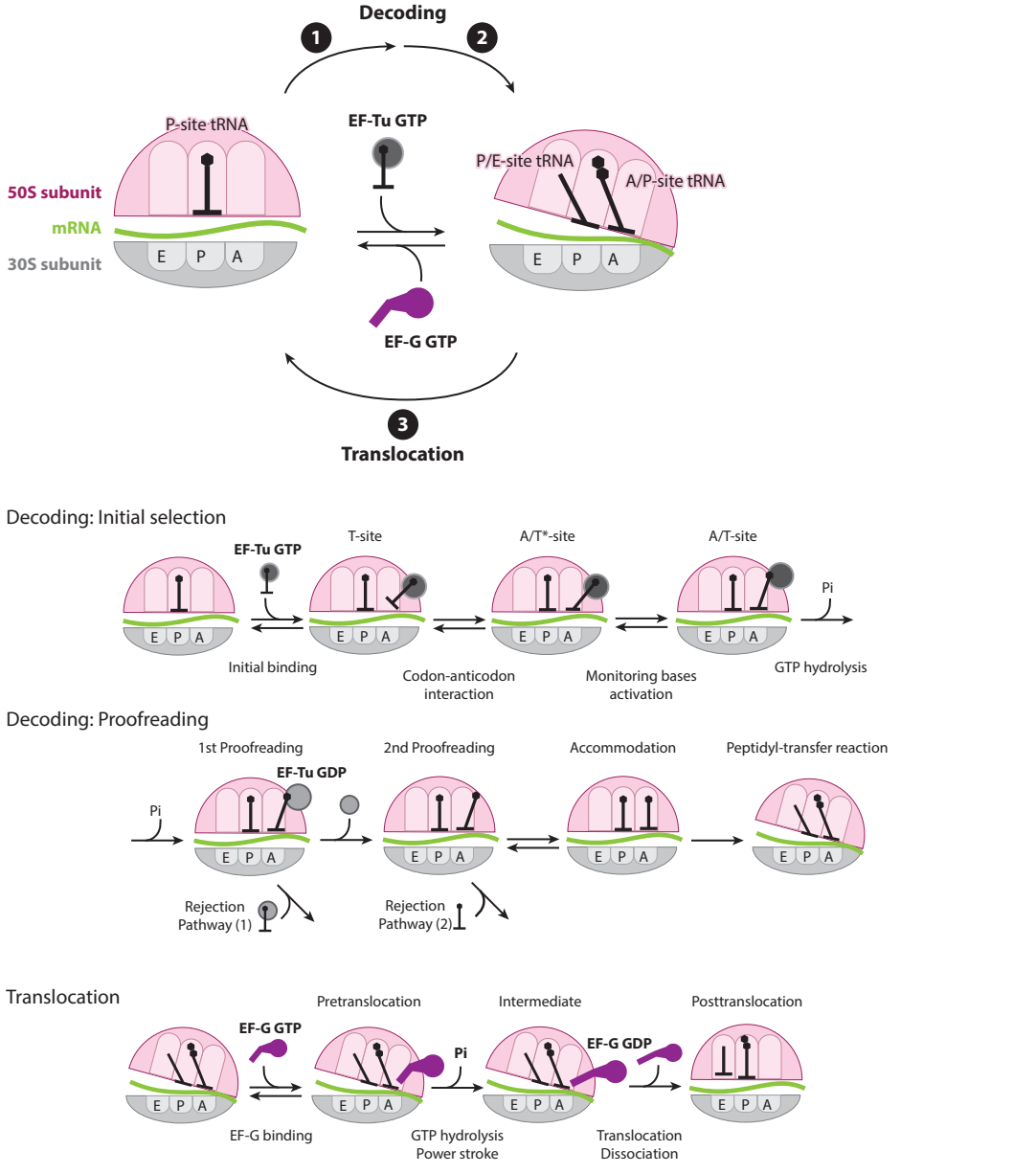

Figure 1

Schematic of translation elongation. (*Top*) For an addition of one amino acid to the growing nascent-peptide chain, the conformation and composition of the ribosome cycle through two global states: First, the A-site codon is decoded via ❶ initial selection and ❷ proofreading by the incoming aminoacyl-tRNA in complex with EF-Tu and GTP. Proofreading ends with the transfer of the nascent peptide to the amino acid on the accommodated tRNA, which is followed by global conformational changes and ❸ translocation (with the help of EF-G complexed with GTP), displaying the next codon in the A site. Abbreviations: EF-G, elongation factor G; EF-Tu, elongation factor Tu; tRNA, transfer RNA.

Figure 2

Different methods used to study translation. The current model of translation elongation has advanced through combining results from different methods to construct a coherent model. Structural methods such as NMR, X-ray crystallography, and cryo-EM provide the structural context of the elongation mechanism at the atomic level. Bulk kinetics methods provide the dynamics links between different biochemical and structural states. Single-molecule fluorescence methods bridge structure and dynamics further by observing both simultaneously. Structures shown are adapted from Reference 16 (PDB IDs: 5UYK, 5UYL, and 5UYM). Bulk kinetics and single-molecule data were adapted from Choi et al. (111). Abbreviations: cryo-EM, cryogenic electron microscopy; EF-Tu, elongation factor Tu; FRET, Förster resonance energy transfer.

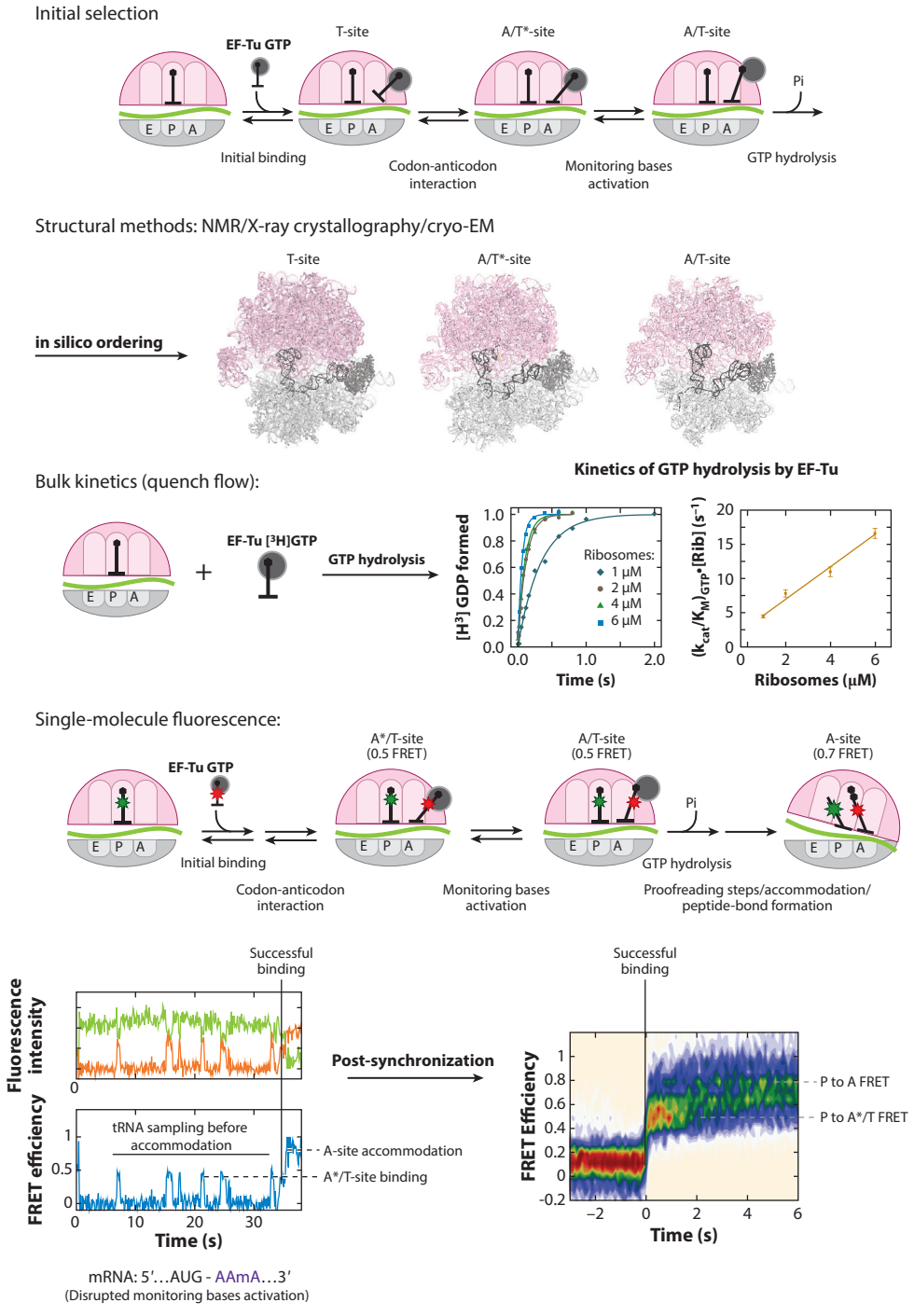

the tRNA dynamically deforms to form a codon-anticodon helix, placing the tRNA in the A*/T state (14). Dynamic formation of the codon-anticodon helix stabilizes tRNA TC binding to the ribosome (20, 24, 52, 53). This is energetically favored for the cognate pairing, which serves to discriminate the noncognate and near-cognate species kinetically before tRNA TC dissociates from the T site (20, 24, 52, 53). Structural methods such as NMR (56) and X-ray crystallography (57, 58) have identified that the correct formation of the codon-anticodon helix leads to activation of the universally conserved monitoring bases (A1492, A1493, and G530 of 16S rRNA within the 30S ribosomal subunit), which dynamically flip toward the codon-anticodon helix and form multiple hydrogen bonds with the *2′-OH* and other conserved chemical groups of the correctly formed helix. The proper interaction among monitoring bases and the codon-anticodon helix positions tRNA TC into the A/T state, providing optimal stereochemistry for the hydrolysis of GTP within the TC through interaction with the sarcin-ricin loop in the 50S ribosomal subunit (58). Recent computational work has shown that the energy landscape of initial selection leading to GTP hydrolysis is markedly different between cognate and near-cognate tRNA bound complexes, where selectivity for the cognate substrate is amplified in multiple steps (20, 52, 53, 59). The irreversible GTP hydrolysis marks the end of the initial selection phase of decoding and subjects the tRNA in the A/T state to additional proofreading steps.

Clever experimental designs using the existing techniques have further elucidated the pathways of translational fidelity through proofreading steps (see **Figure 1**). The proofreading mechanism uses the same stability of codon-anticodon interaction and the monitoring bases conformation to discriminate kinetically against noncognate tRNA species. Recently, bulk-kinetics experiments using engineered tRNAs have suggested that upon GTP hydrolysis, the on-pathway event of EF-Tu•GDP dissociation kinetically competes with the dissociation of EF-Tu•GDP•aa-tRNA, which results in a tRNA rejection pathway (60). Here, the correct stereochemistry among the monitoring bases and the codon-anticodon helix favors the EF-Tu•GDP dissociation pathway over the EF-Tu•GDP•aa-tRNA rejection pathway (60, 61), serving as the first stage of proofreading, although the involved structural mechanism has not been elucidated. Upon EF-Tu•GDP dissociation, aa-tRNA is subjected to the second stage of proofreading, where the on-pathway event of the aa-tRNA accommodation to the A site competes with the dissociation of aa-tRNA from the A/T state. The A-site accommodation places the amino acid moiety of the aa-tRNA in a correct stereochemistry in the peptidyl-transferase center (PTC) of the large ribosomal subunit, which then catalyzes a rapid transfer of the peptide from the P-site tRNA to the amino acid (62).

3.2. Elongation Cycle: Translocation

The peptidyl-transfer reaction after tRNA accommodation induces multiple large-scale conformational changes in the translational complex (63), creating a correct substrate for translocation (see **Figure 1**) (35). Transfer of the nascent peptide to the A-site tRNA allows a movement of the acceptor stems of the P-site and A-site tRNAs into the exit (E) and P sites, respectively, of the large subunit (64). These new tRNA conformations are defined as hybrid states, denoted as P/E and A/P states. In addition to the tRNA movements, peptide-bond formation is also followed by a rapid counterclockwise rotation of the 30S subunit by 3–10° with respect to the 50S subunit, resulting in a rotated-state conformation (65, 66). The rotated-state conformation is the cognate substrate of translocation, catalyzed by an elongation factor [elongation factor G (EF-G) in bacteria and elongation factor 2 (eEF2) in eukaryotes; referred to as EF-G here]. EF-G interacts with the ribosome to stabilize the tRNAs in the hybrid state (21, 67–70). Ribosome binding activates the GTPase of EF-G for GTP hydrolysis (71), leading to its conformational change catalyzing translocation (67–69).

Translocation is by definition dynamic, and many of the intermediate states involved are transient. As such, dynamic methods—bulk kinetics, single-molecule approaches, multiple structures by cryo-EM, computational studies—have been essential for outlining the mechanism of translocation (21, 34, 72–75). Using molecular dynamics simulations, different translocation intermediate structures from cryo-EM have been temporally ordered to build a structural pathway of translocation (76). On the basis of these results, combinations of multiple single-molecule fluorescence signals or fluorescence signals with the measured kinetics from bulk methods have produced detailed models of translocation (21, 34, 74, 75). During translocation, the head of the 30S subunit swivels counterclockwise with respect to the body by 18–21° followed by a rapid relaxation back, coupled with disengagement of the mRNA and tRNAs from the decoding center (72, 73, 77). These changes are also accompanied by a clockwise rotation of the 30S subunit relative to the 50S subunit that places the ribosome back into the nonrotated intersubunit conformation (35, 78, 79). EF-G then dissociates from the nonrotated posttranslocation complex, with tRNAs occupying the P and E sites (80).

After translocation, the dissociation kinetics of deacylated tRNA from the E site determine the structural pathway following translocation. The posttranslocation complex is in the nonrotated conformation with a vacant A site (80), where tRNAs can sample and decode the next codon (25, 81). The decoding process is not allosterically affected by the presence or the absence of the E-site tRNA (25, 81–83). However, upon peptidyl-transfer reaction, deacylated tRNA needs to be moved to the P/E hybrid state for translocation. Thus, E-site occupancy, perhaps due to slow E-site tRNA dissociation kinetics, would preclude adoption of the tRNA hybrid conformation until the E-site tRNA dissociates (36). The E-site tRNA dissociation kinetics are sensitive to intracellular ionic strength (81, 84), temperature, and tRNA identity (36, 85), and they are possibly modulated by additional elongation factors, such as eEF3 in fungi (86, 87) or its bacterial homolog, EF4. More work is required to understand the detailed role of the E site in elongation.

4. MESSENGER RNA ELEMENTS ALTERING TRANSLATION ELONGATION

Beyond their intrinsic capacity to encode proteins, mRNAs possess numerous regulatory elements that impact the rate of protein synthesis at multiple stages. We focus on the increasingly prominent role that the mRNA plays in controlling the rate of elongation. We cover how (*a*) modifications to a single nucleotide, (*b*) codon usage, and (*c*) larger regulatory elements within the mRNA alter translation elongation.

4.1. Nucleotide Modifications

Distinct chemical modifications—163 cataloged to date (88)—have been detected in RNAs. In particular, the past several years have yielded a vast expansion of data that document RNA epigenetics (89) or the mRNA epitranscriptome (90)—the dynamic co- or posttranscriptional addition of modifications to the nucleotides within mRNAs. The epitranscriptome field has moved rapidly, and several excellent reviews have recently been published that highlight recent discoveries around mRNA modifications and the techniques used to identify them (91–94). Modified nucleotides within mRNA have been shown to affect all aspects of RNA biology—mRNA splicing, export, localization, and stability, as well as multiple stages of translation, including elongation (91, 93).

Chemical modifications that occur on nucleotides within the mRNA coding region can be divided into three broad categories (**Figure 3**). First, hydrogen-bonding groups on the nucleotide base can be modified, thereby altering its ability to base-pair with incoming tRNAs. Second,

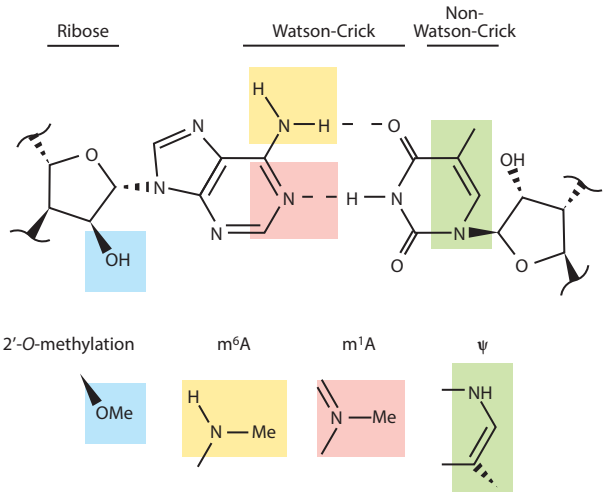

Figure 3

Example of chemical modifications in mRNA. Among hundreds of known chemical modifications of RNA bases, several modifications occurring within the coding region of mRNA can be classified into three categories. First, modifications occurring in the Watson-Crick edge of RNA bases disrupt base-pairing of mRNA (m^6A and m^1A) and hinder secondary structure formation or codon-anticodon interaction. Second, modifications occurring outside the Watson-Crick edges of the base (Ψ) do not alter base-pairing ability of the modified base but could distort the base-pairing of nearby RNA bases. Third, modifications on the ribose of RNA disrupt its interaction with rRNA during decoding (2′-*O*-methylation). Abbreviations: m^1A, N^1-methyladenosine; m^6A, N^6-methyladenosine; mRNA, messenger RNA; rRNA, ribosomal RNA.

the nucleotide base can be modified outside the Watson-Crick edge of the base, without alteration to its hydrogen-bonding ability. Third, the ribose backbone can be modified, which may affect the tertiary structure of mRNA or recognition mechanisms specific to RNA. Each type of modification is expected to induce different effects during decoding, thereby suggesting new ways to regulate the dynamics of translation elongation. In this section, we focus on three known mRNA modifications—methylation of adenosine at the N^6 position (N^6-methyladenosine, m^6A), the isomerization of uracil (pseudouridine, Ψ), and ribose methylation at the 2′ position (2′-*O*-methylation).

m^6A is the most common internal mRNA modification, where one of two N^6 hydrogens that participates in base-pairing is modified to a methyl group (**Figure 3**). Tens of thousands of m^6A sites have been defined in thousands of mRNAs from human, mouse, yeast, plant, and bacterial models (95, 96). Substitution of adenosine nucleotides (A) with m^6A within the open reading frame of mRNAs inhibits translation elongation directly (97). m^6A and U form canonical base-pairs, but they are thermodynamically less stable in duplexes than are canonical A-U base-pairs (98). And, while m^6A base-pairs with the corresponding U in the tRNA anticodon in the ribosomal A site, m^6A at any of the three positions in a codon disrupts decoding, with the greatest kinetic inhibition at the first nucleotide (99). These data suggest that translation kinetics for particular mRNAs in bacteria and eukaryotes could be modulated by dynamic m^6A (de)modifications. Although less common in coding regions (100, 101), N^1-methyladenosine (m^1A) also substantially inhibits tRNA selection and accommodation (102), possibly by preventing codon-anticodon interactions.

The isomerization of uridine to Ψ is the most abundant internal RNA modification, which rearranges atoms outside the Watson-Crick edge (**Figure 3**). In the ribosome, Ψ nucleotides are present in the peptidyl transferase and decoding centers, where they enhance translation efficiency

and fidelity (103, 104). In mRNA, stop codons (UGA, UAA, or UAG) with Ψ as the first nucleotide suppress translation termination and allow read-through of premature termination codons in vitro and in vivo (105, 106). Structural analyses of bacterial 30S ribosomal subunits revealed that the presence of a Ψ-A Watson-Crick base-pair at the first position of a codon-anticodon interaction distorts the conformation of the decoding center (105), allowing typically prohibited noncognate tRNAs to decode the modified stop codon via Hoogsteen base-pairing. However, among hundreds to thousands of Ψ found within the coding regions of eukaryotic mRNAs (107, 108), modifications of stop codons were extremely rare. How sense codons are affected by the presence of Ψ remains unclear and is an exciting avenue for future studies.

Finally, 2′-*O*-methylation is an emerging mRNA modification in eukaryotes. Chemically, by replacing the reactive 2′-*OH* group with an unreactive *O*-methyl group, 2′-*O*-methylation decreases the susceptibility of the nucleotide to nucleolytic attack (i.e., hydrolysis) and stabilizes RNA helices (109). The 2′-*OH* of RNA is a critical contact point in interactions that are specific for RNA over DNA. Thus, 2′-*O*-methylation may have substantial impact on protein-RNA, RNA-RNA, and DNA-RNA interactions. Thousands of 2′-*O*-methylation sites were recently identified within human mRNAs, predominately enriched in the coding region (110). Intriguingly, 2′-*O*-methylation stalls translation elongation at the modified nucleotide during decoding similar to m^6A, with the greatest impact when the codon is 2′-*O*-methylated at position 2 (97, 111). A primary cause of the stall is the disruption of the conserved rRNA monitoring bases, which interact with the mRNA 2′-*O*-moieties for decoding. The distortion of the decoding site leads to both increased rejection of the cognate tRNAs during the initial tRNA selection and subsequent proofreading phases of translation elongation, manifesting as a long stall prior to a successful decoding event. Although the functional role of such a pause has not yet been uncovered, both m^6A and 2′-*O*-methylation in mRNA demonstrate how the rate of translation elongation can be widely tuned by chemical modifications to mRNA.

4.2. Codon Choices Changing Decoding Kinetics and the Pathway of Elongation

Each amino acid is encoded by up to six synonymous codons, and their usage frequencies vary. In many instances, codon usage is optimally balanced with the abundance of the corresponding aa-tRNAs that recognize them (112, 113). Indeed, inclusion of nonoptimal codons inhibits elongation and destabilizes the mRNA (114, 115). The abundance of aa-tRNAs is modulated during cell proliferation and differentiation (116) and in development (117), cancer (118, 119), and other human diseases (120), which together appear to play an important role in regulating the rate of protein synthesis. Thus, seemingly silent DNA mutations that do not impact the encoded amino acid may result in a switch from an optimal to nonoptimal codon (or vice versa), altering the abundance or function of the protein.

Synonymous codon usage has a direct impact on the kinetics of decoding and translocation. The rate of aa-tRNA binding is dictated by both the codon present in the A site and its abundance in a cell (121). The usage of rare codons with low concentrations of corresponding aa-tRNAs thus leads to elongation pauses during the decoding phase. Although the slow decoding rate induced by rare codons may lead to decreased mRNA stability in cells (114, 115), it may also allow domains of the nascent proteins to cotranslationally fold properly; rare codons are especially enriched at the end of protein secondary structures (122). The decoding rate of the A-site codon may be further affected by the codon present in the P site, as permutations of synonymous codons at two adjacent positions contribute to the overall rate of elongation (123). In tandem, the dissociation kinetics of deacylated tRNA from the E site may differ across synonymous codons. Slow E-site tRNA dissociation retains the ribosome in a conformation that is refractory to translocation, where its

lifetime depends on the rate of tRNA dissociation (36). Dissociation kinetics of the E-site tRNA are dependent on the tRNA species (36, 85) and may differ among synonymous codons. We speculate that, together with tRNA abundance, the differential usage of synonymous codons in the A, P, and E sites of the ribosome may lead to nonuniform rates of elongation across an mRNA, which awaits full elucidation.

4.3. Stable RNA Structures Within Messenger RNA

Information encoded in mRNAs occurs in a three-dimensional context. mRNAs can dynamically fold into complex secondary and tertiary structures that may serve as regulatory elements via recruiting factors that recognize RNA structures, disrupting translocation during translation, or modulating more complex translational events on the ribosome.

mRNA structure can be a ligand for translation factors. The incorporation of the twenty-first amino acid, selenocysteine, relies on an RNA-binding protein that specifically recognizes an mRNA stem-loop. A specialized elongation factor (SelB in bacteria, eEFSec-SBP2 in eukaryotes; referred to as SelB) complexed with selenocystenyl-tRNA (Sec-tRNA^{Sec}) and GTP binds to an mRNA stem-loop—the selenocysteine insertion sequence (SECIS) (54). This interaction facilitates timely delivery of Sec-tRNA^{Sec} TC to the ribosomal A site, resulting in the recoding of the UGA stop codon. SECIS is an excellent example of how an mRNA structure and its interaction with an RNA-binding protein can alter decoding.

mRNA structures need to be unfolded prior to decoding by the ribosome. During translation, the single-stranded mRNA is threaded through the 5–6-nucleotide-long entrance channel that is composed of three ribosomal proteins (S3, S4, and S5 in bacteria) (124, 125). The relatively narrow width of the mRNA entrance channel prohibits RNA duplexes from entering. Therefore, structured mRNA elements need to be unfolded approximately two codons before it reaches the A site for decoding (126), possibly during the translocation step. The unfolding of mRNA structure requires free energy, likely powered by EF-G, which hydrolyzes GTP to catalyze translocation. The proposed model of ribosome translocation on an mRNA involves a conformational change in EF-G, which primes the mRNA-tRNA complex for translocation (75, 127). However, the mechanism of translocation through an mRNA hairpin is still debated; although the force generated during the EF-G conformational change may be used directly for helicase activity (75), it has also been suggested that translocation can capture the breathing of the base of the mRNA structure (31). Regardless of the helicase mechanism, mRNA structures have been known to slow down elongation and to be used to enhance recoding efficiency in many cases (2, 22, 128).

mRNA sequences may base-pair with the rRNA to be tethered to the ribosome. The role of mRNA-rRNA base-pairing is a key aspect of bacterial translation initiation and is integral to certain recoding phenomena, such as −1/+1 programmed ribosomal frameshifting (129). However, the mechanism by which mRNA-rRNA base-pairing interactions alter the dynamics of translation elongation has been debated. Early in the study of translation in bacteria, a stretch of mRNA sequence named the Shine-Dalgarno (SD) sequence was recognized as an important feature of translation initiation, guiding the position of the start codon on the ribosome by base-pairing with the small ribosomal subunit. The effect of the SD sequence during elongation surfaced during the study of programmed ribosomal frameshifting, where it has been hypothesized to "push" or "pull" mRNA to aid frameshifting in both directions. However, recent reports have shown that the effect of the SD sequence on translation elongation kinetics may be minimal (130). Therefore, the mechanism by which the SD sequence and similar mRNA-rRNA interactions affect translation and enhance recoding phenomena needs further elucidation.

5. CONTROL OF TRANSLATION ELONGATION BY NASCENT-PEPTIDE ELEMENTS

In addition to mRNA element-mediated regulation, the amino acid sequence of the nascent protein chain also regulates translation (4, 5). Amino acid side-chain geometries and chemistries influence substrate positioning within the PTC (5). In the context of the nascent peptide, amino acids can interact with the ribosomal exit tunnel (an ~100 Å-long conduit that bridges the PTC and the solvent environment), resulting in changes in the rate of translation elongation (4). In this section, we discuss the mechanisms of amino acid sequence-induced ribosomal stalling and its basis in regulating molecular mechanisms such as ribosomal secretion signals and antibiotic resistance.

5.1. Proline-Mediated Translation Stall

The rate of peptidyl transfer for each codon varies depending on how efficient a particular amino acid is as a P-site peptidyl donor and an A-site peptidyl acceptor (131). Proline is the most striking example, given it is the only *N*-alkylated and cyclic proteinogenic amino acid. As the A-site peptidyl acceptor, the transfer reaction to proline is much slower compared with that of other amino acids such as phenylalanine. The higher pKa of the α-*N* group brought about by the alkylation slows down the rate-limiting peptidyl transfer reaction to an A-site proline (132, 133). Recent ribosomal crystal structures with a proline-tRNA analog in the A site revealed unfavorable positioning of the substrate in the PTC (134), which likely further contributes to the slow peptidyl transfer rate of proline. The unfavorable positioning of proline may also explain its poor activity as the peptidyl donor in the ribosomal P site (135). The low reactivity of proline in both A and P sites results in an amplified inhibition of translating consecutive proline (136, 137).

Proline residues can therefore potentially regulate the rate of protein synthesis. The stalling caused by stretches of proline residues can be alleviated by a special elongation factor [elongation factor P (EF-P) in bacteria and initiation factor 5A (eIF5A) in eukaryotes; referred to as EF-P here] (135, 138, 139), by decreasing the activation energy for formation of the next peptide bond via a favorable entropy change (140). Ribo-Seq results revealed significant ribosomal stalling events at the poly-Pro regions in mRNAs when EF-P was knocked out (141), reflecting the direct effect of EF-P/poly-Pro on mRNA translation. The recent cryo-EM structure of EF-P bound to the stalled ribosome suggested that EF-P stabilizes conformation of the nascent peptide and tRNAs to allow efficient translation of poly-Pro regions (142). Combined with cellular levels of EF-P, stretches of proline residues directly affect the expression levels of the corresponding proteins, especially those involved in the synthesis of key components of the translation machinery; this may in turn act as an indirect regulator for the translation of other mRNAs or global protein synthesis (143, 144).

5.2. Effects of Interactions Within the Nascent-Peptide Exit Tunnel on Translation Elongation

Unlike proline residues, which require interaction with only the PTC to induce translational stalling, there are longer nascent-peptide sequences that can arrest translating ribosomes through specific interactions with the constricted region of the ribosomal exit tunnel (4). One of the most extensively studied examples of nascent-chain-induced stalling is the *secM/secA* ribosomal secretion signaling pathway in bacteria (145). Expression of the SecA protein is coupled to the cellular protein secretion pathway via a negative feedback mechanism, where inefficiencies in the secretion pathway involving SecA induce increased translation of the *secA* gene. The mechanism

of such modulation involves the translation of a secretory protein, SecM, which acts to monitor the efficiency of protein export. SecM includes a nascent-peptide sequence that induces a stall in translation, which is relieved when the SecM-stalled ribosomes are docked to the Sec translocon on the cell membrane via the SecA-mediated protein secretion pathway. The *secA* initiation site is located in the 3′-UTR of *secM* and, under normal conditions, is structurally sequestered away from ribosomal binding (**Figure 4**). The prolonged translation stalling on SecM rearranges mRNA structures to expose the initiation site of the *secA* gene and thus prompts the synthesis of the SecA protein.

Biochemical and genetic studies have identified a 17-aa peptide in SecM, F^{150}XXXXWIXXXXGIRAGP^{166} (145), that is sufficient for stalling translating ribosomes at Gly^{165} (146). Structural studies by cryo-EM showed how interactions between the SecM-stalling peptide and the ribosomal exit tunnel affect positioning of substrates in the PTC and slow down the peptidyl transfer reaction between Gly^{165} and Pro^{166} (147). Disruption in the PTC and interaction within the nascent-peptide exit tunnel may affect translocation as well as the peptidyl transfer reaction. Using cryo-EM, Zhang et al. (148) captured not only the inactive PTC state that disfavored the accommodation of the incoming A-site tRNA and peptide-bond formation, but also another state where the translocation was impaired after successful peptide-bond formation. Recent single-molecule studies uncovered the real-time dynamic nature of this stalling phenomenon, which involves prolonged decoding and translocation at several positions in SecM (149). This work suggests that residues in SecM interact cooperatively with the ribosome to induce a gradual slow-down of translation elongation. The gradual slow-down of elongation suggests multiple interactions between the nascent peptide and the ribosome, which evolve over the course of translating a SecM-stalling peptide (**Figure 4**).

Other peptide sequences with moderate effects on ribosomal stalling may be used more pervasively to regulate biomolecular processes. To date, many translation stalling peptide sequences have been identified (4). New methods for identifying peptide sequences that induce translational stalling continue to be developed: Using bioinformatics, Navon et al. (150) identified underrepresented short-peptide sequences that indeed stall translation. Through genetic selection, Tanner et al. (151) evolved a novel peptide sequence, FXXYXIWPP, that impairs peptidyl transfer, causing translating ribosomes to stall. How different nascent-peptide elements are used to induce perturbation in decoding and/or translocation kinetics in prokaryotic and eukaryotic elongation still needs further clarification.

5.3. Sequence-Context-Dependent Action of Antibiotics

Many antibiotics target key functions of translation by interacting with active sites within the ribosome. Certain classes of antibiotics specifically impede the peptidyl-transfer reaction (152), whereas others, such as macrolides like erythromycin, bind to the ribosomal exit tunnel and cause ribosomal stalling and abortive translation (153). Initial studies suggested that erythromycin acted as a plug in the ribosome exit tunnel blocking the passage of the nascent peptide. However, recent results indicate that the erythromycin mechanism of action relies on the interplay between the nascent peptide, the tunnel, and the drug itself, whereas the susceptibility to the drug depends on the nascent-peptide sequence (154, 155). Similarly, the actions of different antibiotics such as chloramphenicol and linezolid have also been shown to depend on the distinctive nascent-peptide sequence, leading to stable accommodation events of incoming tRNA but preventing peptide-bond formation on the stalling site only (156). Bound antibiotics likely interact with nascent-peptide residues to disrupt the PTC, which affects the accommodation dynamics of the next A-site tRNA and results in abortive translation.

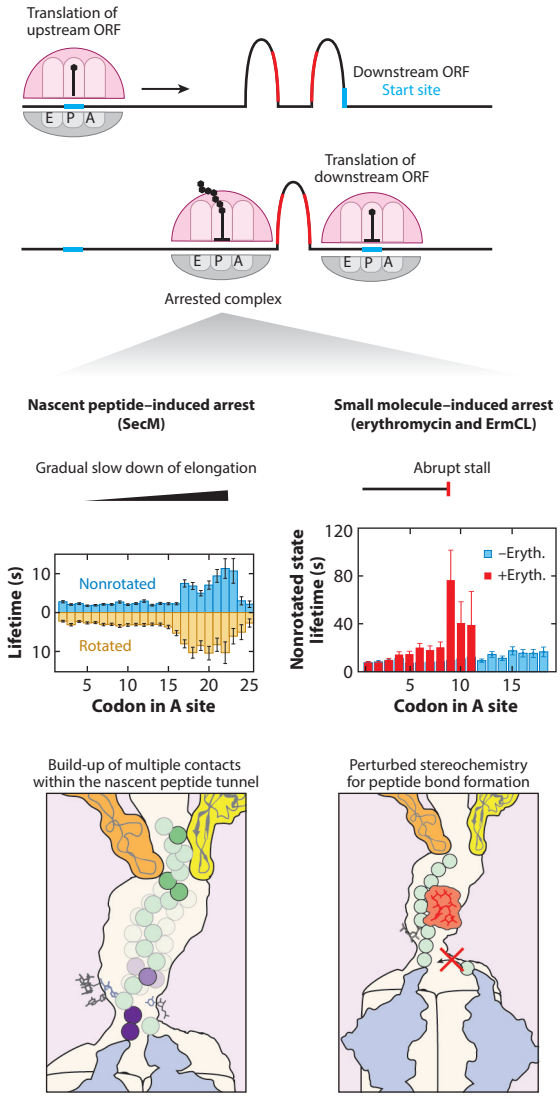

Figure 4

Interactions within the NPET modulate translation dynamics. Various nascent-peptide elements are known to stall translation of the upstream ORF at a precise location to induce rearrangements of mRNA folding and expose the previously sequestered translation start site of the downstream ORF. The stall can be induced by nascent-peptide elements only, some of which have been shown to slow down elongation gradually by building multiple contacts within the NPET as the nascent peptide is extended. In addition, interactions with a small molecule can cause an abrupt stall of translation at one codon. Single-molecule data and graphics of NPET were adapted from References 149 and 154. Abbreviations: mRNA, messenger RNA; NPET, nascent-peptide exit tunnel; ORF, open reading frame.

Translational inhibition is blocked through mechanisms of antibiotic resistance. For erythromycin, the basis for the regulation of resistance is similar to the translational attenuation principle as described above for *secM-secA* gene regulation. The activation of the macrolide resistance gene *ermC* relies on translational stalling on the upstream *ermCL* gene to upregulate protein synthesis (157). The *ermCL* gene harbors a specific nascent-peptide sequence that induces a strong translational arrest in the presence of the erythromycin (**Figure 4**) (153, 154, 158). The stalled ribosome induces a rearrangement of mRNA structures to expose the initiation site of the downstream *ermC* gene and upregulates the expression level of the ErmC methyltransferase (**Figure 4**) (157). The translation of *ermC* confers antibiotic resistance by methylation of A2058 of 23S rRNA (159), which likely disrupts the binding of the erythromycin to the ribosome. Similarly, a strong chloramphenicol-dependent stall-inducing nascent-peptide sequence is present in the *catA86L* or *cmlAL* genes to upregulate expression of the downstream *catA86* or *cmlA* genes to confer resistance to chloramphenicol (160). A nascent-peptide sequence can also confer antibiotic resistance for translating individual proteins, where bound antibiotics are evicted through interactions with the growing nascent chain (154, 161). Although distinct interactions of the nascent chain, the exit tunnel and the small molecules are employed in different drug actions, these studies underscore how such interactions can modulate translation dynamics. Therefore, a dynamic view of translation is necessary for understanding the mechanisms of antibiotics and the development of resistance.

6. RECODING

The existence of multiple mRNA and nascent-peptide elements that affect translation elongation at various steps highlights the flexibility of the translation machinery to utilize different signals encoded in the mRNA. Individually, the major effect of mRNA and nascent-peptide elements is to modulate the rate of translation elongation. However, combinations of multiple effects may break the linearity of elongation and bifurcate its pathway to produce two different proteins in a tuned ratio from the same mRNA, which is referred to as recoding events. Across the domains of life, different genes utilize recoding signals to increase the density of their genetic information or to regulate the production of a functional protein. In recoding, the normal elongation pathway competes with the recoded pathway, and determining the exact branch point of pathways is critical in elucidating the mechanism of specific recoding phenomena. Different branching points involved in the various recoding phenomena are starting to be exposed, occurring during either translocation or decoding steps, or a combination of both in the extreme case (**Figure 5**).

6.1. The Repurposing of Translocation for −1 Frameshifting

Programmed ribosomal −1 frameshifting (referred to as −1 frameshifting) is the best-studied recoding phenomenon to date. During −1 frameshifting, the open reading frame of the mRNA contains a programmed "slippery sequence": a sequence of nucleotides where translation can resume in the original frame (0 frame) or in another shifted one base in the 5′ direction (−1 frame). Translation of a −1 frameshifting signal thus produces two different proteins that share the same N-terminal sequence with a fixed stoichiometry. The most well-known usage of −1 frameshifting is in human immunodeficiency virus (HIV), where a −1 frameshifting signal is used to produce Gag and Gag-Pol proteins at a predetermined ratio (1). Regulating protein expressions through −1 frameshifting enriches the information density of genomes and likely benefits viruses such as HIV, where the fitness of a virus is linked to the compactness of its genome. New instances of −1 frameshifting are still being discovered in viruses, bacteria, and eukaryotes, and its usage may

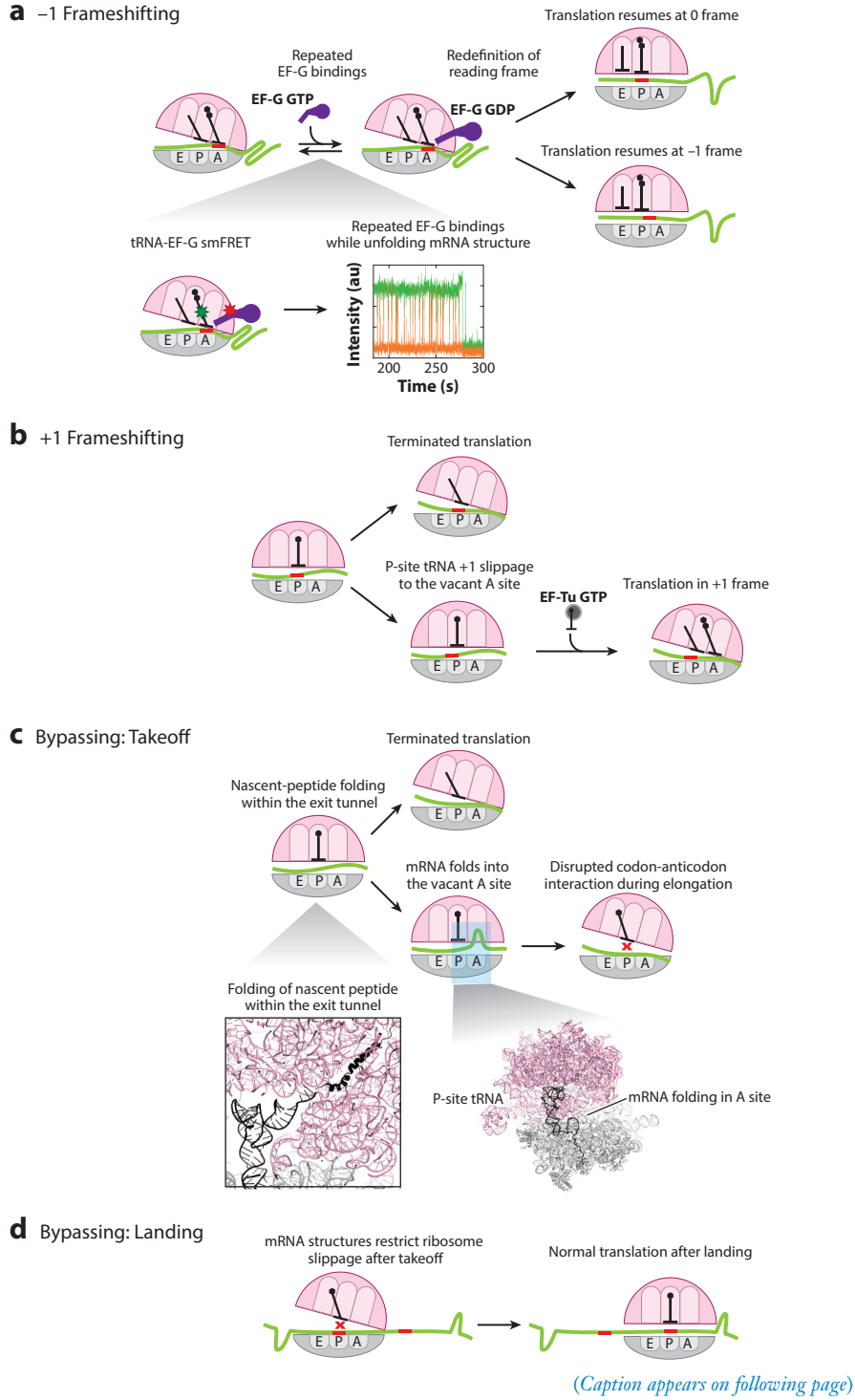

(*Caption appears on following page*)

Figure 5 (*Figure appears on preceding page*)

Mechanisms of recoding events involving disrupted translocation and decoding. (*a*) −1 Frameshifting is likely to occur during translocation, impeded by mRNA structure. Translocation into the structured region of mRNA leads to multiple futile bindings of EF-G (shown from smFRET experiments), which may hydrolyze GTP to translocate the codon-anticodon helix and unfold the mRNA structure simultaneously. The EF-G-bound state may be susceptible to the frameshifting prior to translocation. (*b*) +1 Frameshifting may occur during inefficient decoding, where the A-site substrate in the +1 frame (aa-tRNA ternary complex) may compete with the A-site substrate in the original frame (release factors or another aa-tRNA ternary complex). Intermediate structures and dynamics of +1 frameshifting have yet to be revealed. (*c*) The first stage of bypassing involves impeded decoding by the folding of the nascent-peptide chain within the exit tunnel, which allows mRNA to fold into the vacant A site and weaken codon-anticodon interactions in the P site, facilitating the takeoff of the ribosome from the current P-site codon. The structures shown were adapted from Reference 181. (*d*) After takeoff, landing of the ribosome during bypassing may involve several mRNA structures that limit the translocation of the taken-off ribosome. Repeated EF-G binding during landing has been observed in smFRET experiments; however, the role of EF-G during landing is still unclear. Abbreviations: aa-tRNA, aminoacyl-tRNA; EF-G, elongation factor G; mRNA, messenger RNA; smFRET, single-molecule Förster resonance energy transfer; tRNA, transfer RNA.

be much higher than anticipated, perhaps stimulated by external elements such as RNA-binding proteins (162), microRNAs (163), and antibiotics (164).

Translation normally requires ribosomes to maintain their original reading frame throughout elongation. Errors resulting from the spontaneous shifting of the reading frame are energetically costly, resulting in the production of unwanted proteins that may be harmful to the cell. The error rate for the spontaneous shifting has been estimated as 10^{-5} (165, 166), which is an order of magnitude smaller than the 10^{-4} rate of missense errors (substitution of a single amino acid) (167, 168). Therefore, −1 frameshifting signals that result in 30–70% efficiency present a controlled way to circumvent an error prevention mechanism utilized during normal elongation (1–3).

The set of factors involved in −1 frameshifting is continually expanding and includes both mRNA and nascent-peptide elements, as well as external factors. Among them, the slippery sequence within the mRNA is essential. They typically conform to a tetrameric or heptameric sequence (N–NNX–XXZ or X–XXX–XXZ, where N, X, and Z denote a nucleotide, and a dash denotes separation of codons in the original reading frame) that allows cognate tRNA pairing in two frames. The heptameric sequence generally yields higher frameshifting efficiency than that of the tetrameric sequence, indicating that it can involve up to two tRNAs (169).

However, the slippery sequence alone does not induce highly efficient −1 frameshifting—usually less than 5% (1–3, 170, 171). Downstream mRNA structures are most often required for highly efficient −1 frameshifting of up to 50–70% (1–3, 170, 171). The involved structures are strikingly varied, from a simple stem-loop to a pseudoknot to long-range RNA folding that spans distances of thousands of nucleotide bases within a single mRNA molecule (1–3). The stability of the RNA structures positively correlates with −1 frameshifting efficiency (171). Moreover, microRNAs (162) and RNA-binding proteins (162) enhance −1 frameshifting efficiency, very likely by increasing the stability of the mRNA structure. In addition to the stability of the mRNA structure, its position relative to the slippery sequence also affects −1 frameshifting. Highly efficient frameshifting systems frequently contain 5–6 nucleotides between the 3′ end of the slippery sequence and the 5′ base of the mRNA structure. Deviation from this distance in either direction decreases frameshifting efficiency (128, 170).

The mechanism of −1 frameshifting is emerging from a combination of different methods. Through studies of individual mRNA structures used in −1 frameshifting, it is clear that they act to induce a pause during translation elongation. The pause most likely occurs during translocation

(22, 172, 173), requiring multiple EF-G bindings to catalyze translocation on the slippery sequence coupled with the simultaneous unfolding of the mRNA structure (**Figure 5*a***). Indeed, the distance of 5–6 nucleotides between the slippery sequence and the mRNA structure matches the length of the mRNA entrance channel (124, 125). Furthermore, this distance induces a substantially longer translocation pause than the same structure placed 7 nucleotides away from the slippery sequence (126).

Within the translation elongation cycle, translocation poses a unique opportunity for −1 frameshifting. During translocation, the ribosome needs to transfer tRNA-mRNA complexes from one position (A/P and P/E) to another (P and E) (73). This transition must disrupt all existing interactions between the tRNA-mRNA complex and the ribosome, specifically on the 30S ribosomal subunit. Thus, at this point in translation, the reading frame is particularly vulnerable to spontaneous shifts. The slippery sequence may act to lower the energy barrier for such spontaneous shifts toward one direction in the translocation intermediate state, whereas the mRNA structure may act to increase the lifetime of such a state (172, 173). The transition state may require binding of EF-G and its conformational change after GTP hydrolysis (75), which may be necessary to weaken the tRNA-mRNA/ribosome interaction (77). This suggests that the −1 frameshifting mechanism repurposes futile translocation cycles catalyzed by EF-G during the unfolding of the mRNA structure, to traverse the frameshifting energy barrier.

The link between repeated translocation attempts on the slippery sequence and −1 frameshifting explains the use of different factors to enhance −1 frameshifting efficiency. The nascent-peptide signal can also disrupt translocation and induce multiple translocation attempts by EF-G (149), which may act in a similar manner as the mRNA structure to increase −1 frameshifting efficiency. The presence of antibiotics such as telithromycin may increase the efficiency of −1 frameshifting by mimicking such nascent-peptide signals (154, 164). On poly-A mRNA sequences, repeated A–AAA–AAA sequences can act as slippery sequences, and multiple translocations from one slippery sequence to the next may explain the high occurrences of frameshifting at these locations that signal aberrant translation happening in the untranslated region (174, 175). Finally, the energy barrier for spontaneous frameshifting on the slippery sequence depends not only on the composition of the slippery sequence itself, but also on external elements. Particularly, the internal SD sequence may induce a force to alter its free energy barrier height and facilitate −1 frameshifting (170). Taken together, the −1 frameshifting cassette repurposes the translocation force, which is used to unfold mRNA structures or disengage interactions within the nascent-peptide exit tunnel, to redefine the reading frame of the actively translating ribosome.

6.2. Disruption of Decoding by Messenger RNA Used in +1 Frameshifting

Although −1 frameshifting illustrates the use of mRNA and nascent-peptide elements to induce recoding by disrupting translocation, the mechanism of other recoding phenomena, such as +1 frameshifting and bypassing, may exploit delayed decoding. Programmed +1 frameshifting was first identified in the *prfB* gene of *Escherichia coli*, which encodes for release factor 2 (RF2) that recognizes UGA and UAA stop codons for translation termination. However, the RF2 sequence is encoded in the +1 reading frame (shifted one base toward the mRNA 3′ direction) with respect to its initiation site, requiring +1 frameshifting to bypass the internal UGA stop codon in the 0 frame. In fact, the +1 frameshifting occurs at a slippery sequence (CUU-UGA) next to the stop codon, which allows cognate pairing of $tRNA^{Leu}$ (with the AAG anticodon) in two frames (129). In addition to the slippery sequence, a nearby strong SD sequence enhances +1 frameshifting efficiency as well. However, the strongest modulator of +1 frameshifting efficiency on *prfB* is the intracellular concentration of RF2 itself (176), where its high concentration inhibits +1 frameshifting efficiency.

This suggests that the absence of the cognate substrate (aa-tRNA or RF2) in the A site may make the ribosome more susceptible to +1 frameshifting. The mechanism of *prfB* +1 frameshifting presents a negative feedback system to control the concentration of RF2, where its absence promotes +1 frameshifting to synthesize more copies of RF2. Although the report of +1 frameshifting occurrence in other systems has been sparse, recent reports suggested that +1 frameshifting occurs pervasively in some *Euplotes* species, where the stop codon again signals +1 or +2 frameshifting instead of termination, possibly related to kinetic competition between 0-frame and +1- or +2-frame A-site substrates (**Figure 5*b***) (177, 178).

6.3. Disruption of Decoding and Translocation Used in Bypassing

Translational bypassing is a spectacular and striking example of recoding, involving an interplay of mRNA structure and nascent-peptide chain interactions. During bypassing observed in *gene 60* of T4 bacteriophage, a population of the translating ribosomes is detached from the codon-anticodon interaction ("takeoff") to hop a stretch of nucleotides in the coding region and resume translation at a downstream matching codon ("landing") (6, 179). Among the factors utilized to enhance bypassing, the nascent-peptide sequence has been suggested to serve dual roles during bypassing (**Figure 5*c***). First, its interaction with the nascent-peptide exit tunnel may prevent peptidyl-tRNA from dissociation once the codon-anticodon interaction has been disrupted during takeoff. Second, the nascent peptide may disrupt the decoding dynamics similar to the *SecM* sequence (180) to keep the ribosomal A site vacant. Recent cryo-EM and single-molecule studies have shown that a small mRNA structure can form within the vacant A site (**Figure 5*c***) (180, 181), which has been suggested to disrupt the codon-anticodon interaction prior to takeoff. The A site codon is the UAG stop codon, which may prolong the vacancy in the A site similar to +1 frameshifting.

Once the ribosome has broken the codon-anticodon interaction in the P site during takeoff, it needs to translocate to find the correct landing site. Prior to landing, the ribosome is likely to be in the rotated-like state, observed using smFRET methods, where EF-G-catalyzed translocation is inhibited (**Figure 5*d***) (180). In addition to the nascent-peptide element and mRNA structure forming in the A site, bypassing may involve two more mRNA structures, which may act to book-end the slippage of ribosomes after takeoff (180, 182). However, it is less likely that these mRNA structures disrupt translocation to enhance bypassing efficiency, unlike what has been observed in −1 frameshifting. The rotated-like state is resolved once the ribosome finds its correct landing site, where normal elongation resumes (180). The different uses of the same mRNA and nascent-peptide elements observed across different recoding phenomena demonstrate the flexibility of the translational machinery, and the enrichment of genetic codes during protein synthesis.

7. CONCLUSIONS AND PERSPECTIVES

Myriad ways of controlling translation elongation dynamics have been revealed during the past decades, with more surely to be uncovered. This review has focused on how the core substrate and product of translation—mRNA and protein—can act as modulators of the overall process. The molecular and dynamic complexity of translation will continue to challenge our ability to capture mechanistic detail with atomic precision. However, the promising confluence of structural, dynamic, and genomic and proteomic methods bodes well for our ability to unravel this complexity. Technological advances in instrumentation sensitivity and computational power underlie this progress; understanding the central role of translation in health and disease requires it.

DISCLOSURE STATEMENT

The authors are not aware of any affiliations, memberships, funding, or financial holdings that might be perceived as affecting the objectivity of this review.

LITERATURE CITED

1. Atkins JF, Gesteland RF, eds. 2010. *Recoding*: *Expansion of Decoding Rules Enriches Gene Expression*. New York: Springer Verlag
2. Caliskan N, Peske F, Rodnina MV. 2015. Changed in translation: mRNA recoding by −1 programmed ribosomal frameshifting. *Trends Biochem. Sci.* 40(5):265–74
3. Atkins JF, Loughran G, Bhatt PR, Firth AE, Baranov PV. 2016. Ribosomal frameshifting and transcriptional slippage: from genetic steganography and cryptography to adventitious use. *Nucleic Acids Res.* 44(15):7007–78
4. Ito K, Chiba S. 2013. Arrest peptides: cis-acting modulators of translation. *Annu. Rev. Biochem.* 82:171–202
5. Wilson DN, Arenz S, Beckmann R. 2016. Translation regulation via nascent polypeptide-mediated ribosome stalling. *Curr. Opin. Struct. Biol.* 37:123–33
6. Weiss RB, Huang WM, Dunn DM. 1990. A nascent peptide is required for ribosomal bypass of the coding gap in bacteriophage T4 gene 60. *Cell* 62(1):117–26
7. Meydan S, Klepacki D, Karthikeyan S, Margus T, Thomas P, et al. 2017. Programmed ribosomal frameshifting generates a copper transporter and a copper chaperone from the same gene. *Mol. Cell.* 65(2):207–19
8. Mustoe AM, Brooks CL, Al-Hashimi HM. 2014. Hierarchy of RNA functional dynamics. *Annu. Rev. Biochem.* 83:441–66
9. Javed A, Christodoulou J, Cabrita LD, Orlova EV. 2017. The ribosome and its role in protein folding: looking through a magnifying glass. *Acta Crystallogr. Sect. D.* 73(6):509–21
10. Nygaard R, Romaniuk JAH, Rice DM, Cegelski L. 2017. Whole ribosome NMR: dipolar couplings and contributions to whole cells. *J. Phys. Chem. B.* 121(40):9331–35
11. Gelis I, Vitzthum V, Dhimole N, Caporini MA, Schedlbauer A, et al. 2013. Solid-state NMR enhanced by dynamic nuclear polarization as a novel tool for ribosome structural biology. *J. Biomol. NMR.* 56(2):85–93
12. Kurauskas V, Crublet E, Macek P, Kerfah R, Gauto DF, et al. 2016. Sensitive proton-detected solid-state NMR spectroscopy of large proteins with selective CH_3 labelling: application to the 50S ribosome subunit. *Chem. Commun.* 52(61):9558–61
13. Barbet-Massin E, Huang CT, Daebel V, Hsu STD, Reif B. 2015. Site-specific solid-state NMR studies of "trigger factor" in complex with the large ribosomal subunit 50S. *Angew. Chem. Int. Ed.* Engl. 54(14):4367–69
14. Voorhees RM, Ramakrishnan V. 2013. Structural basis of the translational elongation cycle. *Annu. Rev. Biochem.* 82:203–36
15. Liu Z, Gutierrez-Vargas C, Wei J, Grassucci RA, Sun M, et al. 2017. Determination of the ribosome structure to a resolution of 2.5 Å by single-particle cryo-EM. *Protein Sci.* 26(1):82–92
16. Loveland AB, Demo G, Grigorieff N, Korostelev AA. 2017. Ensemble cryo-EM elucidates the mechanism of translation fidelity. *Nature* 546(7656):113–17
17. Fischer N, Neumann P, Konevega AL, Bock LV, Ficner R, et al. 2015. Structure of the *E. coli* ribosome-EF-Tu complex at <3Å resolution by C_s-corrected cryo-EM. *Nature* 520(7548):567–70
18. Chen B, Kaledhonkar S, Sun M, Shen B, Lu Z, et al. 2015. Structural dynamics of ribosome subunit association studied by mixing-spraying time-resolved cryogenic electron microscopy. *Structure* 23(6):1097–1105
19. Shaikh TR, Yassin AS, Lu Z, Barnard D, Meng X, et al. 2014. Initial bridges between two ribosomal subunits are formed within 9.4 milliseconds, as studied by time-resolved cryo-EM. *PNAS* 111(27):9822–27
20. Johansson M, Bouakaz E, Lovmar M, Ehrenberg M. 2008. The kinetics of ribosomal peptidyl transfer revisited. *Mol. Cell.* 30(5):589–98

21. Belardinelli R, Sharma H, Caliskan N, Cunha CE, Peske F, et al. 2016. Choreography of molecular movements during ribosome progression along mRNA. *Nat. Struct. Mol. Biol.* 23(4):342–48
22. Caliskan N, Katunin VI, Belardinelli R, Peske F, Rodnina MV. 2014. Programmed -1 frameshifting by kinetic partitioning during impeded translocation. *Cell* 157(7):1619–31
23. Wang J, Kwiatkowski M, Forster AC. 2015. Kinetics of ribosome-catalyzed polymerization using artificial aminoacyl-tRNA substrates clarifies inefficiencies and improvements. *ACS Chem. Biol.* 10(10):2187–92
24. Blanchard SC, Gonzalez RL, Kim HD, Chu S, Puglisi JD. 2004. tRNA selection and kinetic proofreading in translation. *Nat. Struct. Mol. Biol.* 11(10):1008–14
25. Uemura S, Aitken CE, Korlach J, Flusberg BA, Turner SW, Puglisi JD. 2010. Real-time tRNA transit on single translating ribosomes at codon resolution. *Nature* 464(7291):1012–17
26. Marshall RA, Aitken CE, Dorywalska M, Puglisi JD. 2008. Translation at the single-molecule level. *Annu. Rev. Biochem.* 77:177–203
27. Frank J, Gonzalez RL. 2010. Structure and dynamics of a processive Brownian motor: the translating ribosome. *Annu. Rev. Biochem.* 79:381–412
28. Wang Y, Qin H, Kudaravalli RD, Kirillov SV, Dempsey GT, et al. 2007. Single-molecule structural dynamics of EF-G-ribosome interaction during translocation. *Biochemistry* 46(38):10767–75
29. Munro JB, Altman RB, O'Connor N, Blanchard SC. 2007. Identification of two distinct hybrid state intermediates on the ribosome. *Mol. Cell.* 25(4):505–17
30. Fei J, Kosuri P, MacDougall DD, Gonzalez RL. 2008. Coupling of ribosomal L1 stalk and tRNA dynamics during translation elongation. *Mol. Cell.* 30(3):348–59
31. Qu X, Wen J-D, Lancaster L, Noller HF, Bustamante C, Tinoco I. 2011. The ribosome uses two active mechanisms to unwind messenger RNA during translation. *Nature* 475(7354):118–21
32. Comstock MJ, Ha T, Chemla YR. 2011. Ultrahigh-resolution optical trap with single-fluorophore sensitivity. *Nat. Methods.* 8(4):335–40
33. Roy R, Hohng S, Ha T. 2008. A practical guide to single-molecule FRET. *Nat. Methods.* 5(6):507–16
34. Wasserman MR, Alejo JL, Altman RB, Blanchard SC. 2016. Multiperspective smFRET reveals rate-determining late intermediates of ribosomal translocation. *Nat. Struct. Mol. Biol.* 23(4):333–41
35. Chen J, Petrov A, Tsai A, O'Leary SE, Puglisi JD. 2013. Coordinated conformational and compositional dynamics drive ribosome translocation. *Nat. Struct. Mol. Biol.* 20(6):718–27
36. Choi J, Puglisi JD. 2017. Three tRNAs on the ribosome slow translation elongation. *PNAS* 114(52):13691–96
37. Ingolia NT, Ghaemmaghami S, Newman JRS, Weissman JS. 2009. Genome-wide analysis in vivo of translation with nucleotide resolution using ribosome profiling. *Science* 324(5924):218–23
38. Brar GA, Weissman JS. 2015. Ribosome profiling reveals the what, when, where and how of protein synthesis. *Nat. Rev. Mol. Cell Biol.* 16(11):651–64
39. McGlincy NJ, Ingolia NT. 2017. Transcriptome-wide measurement of translation by ribosome profiling. *Methods* 126:112–29
40. Jan CH, Williams CC, Weissman JS. 2014. Principles of ER cotranslational translocation revealed by proximity-specific ribosome profiling. *Science* 346(6210):1257521
41. Bartholomäus A, Del Campo C, Ignatova Z. 2016. Mapping the non-standardized biases of ribosome profiling. *Biol. Chem.* 397(1):23–35
42. Van Dijk EL, Jaszczyszyn Y, Thermes C. 2014. Library preparation methods for next-generation sequencing: Tone down the bias. *Exp. Cell Res.* 322(1):12–20
43. Gonzalez C, Sims JS, Hornstein N, Mela A, Garcia F, et al. 2014. Ribosome profiling reveals a cell-type-specific translational landscape in brain tumors. *J. Neurosci.* 34(33):10924–36
44. Chen J, Choi J, O'Leary SE, Prabhakar A, Petrov A, et al. 2016. The molecular choreography of protein synthesis: translational control, regulation, and pathways. *Q. Rev. Biophys.* 49:e11
45. Simms CL, Thomas EN, Zaher HS. 2017. Ribosome-based quality control of mRNA and nascent peptides. *Wiley Interdiscip. Rev. RNA.* 8(1):e1366
46. Buskirk AR, Green R. 2017. Ribosome pausing, arrest and rescue in bacteria and eukaryotes. *Philos. Trans. R. Soc. B* 372(1716):20160183

47. Joazeiro CAP. 2017. Ribosomal stalling during translation: providing substrates for ribosome-associated protein quality control. *Annu. Rev. Cell Dev. Biol.* 33:343–68
48. Brandman O, Hegde RS. 2016. Ribosome-associated protein quality control. *Nat. Struct. Mol. Biol.* 23(1):7–15
49. Defenouillère Q, Fromont-Racine M. 2017. The ribosome-bound quality control complex: from aberrant peptide clearance to proteostasis maintenance. *Curr. Genet.* 63(6):997–1005
50. Ninio J. 1975. Kinetic amplification of enzyme discrimination. *Biochimie* 57(5):587–95
51. Hopfield JJ. 1974. Kinetic proofreading: a new mechanism for reducing errors in biosynthetic processes requiring high specificity. *PNAS* 71(10):4135–39
52. Gromadski KB, Rodnina MV. 2004. Kinetic determinants of high-fidelity tRNA discrimination on the ribosome. *Mol. Cell.* 13(2):191–200
53. Gromadski KB, Daviter T, Rodnina MV. 2006. A uniform response to mismatches in codon-anticodon complexes ensures ribosomal fidelity. *Mol. Cell.* 21(3):369–77
54. Fischer N, Neumann P, Bock LV, Maracci C, Wang Z, et al. 2016. The pathway to GTPase activation of elongation factor SelB on the ribosome. *Nature* 540(7631):80–85
55. Rodnina MV, Gromadski KB, Kothe U, Wieden HJ. 2005. Recognition and selection of tRNA in translation. *FEBS Lett.* 579(4):938–42
56. Yoshizawa S, Fourmy D, Puglisi JD. 1999. Recognition of the codon-anticodon helix by ribosomal RNA. *Science* 285(5434):1722–25
57. Ogle JM, Brodersen DE, Clemons WM, Tarry MJ, Carter AP, Ramakrishnan V. 2001. Recognition of cognate transfer RNA by the 30S ribosomal subunit. *Science* 292(5518):897–902
58. Ogle JM, Murphy FV, Tarry MJ, Ramakrishnan V. 2002. Selection of tRNA by the ribosome requires a transition from an open to a closed form. *Cell* 111(5):721–32
59. Satpati P, Sund J, Åqvist J. 2014. Structure-based energetics of mRNA decoding on the ribosome. *Biochemistry* 53(10):1714–22
60. Ieong K-W, Uzun Ü, Selmer M, Ehrenberg M. 2016. Two proofreading steps amplify the accuracy of genetic code translation. *PNAS* 113:13744–49
61. Noel JK, Whitford PC. 2016. How EF-Tu can contribute to efficient proofreading of aa-tRNA by the ribosome. *Nat. Commun.* 7:13314
62. Beringer M, Rodnina MV. 2007. The ribosomal peptidyl transferase. *Mol. Cell.* 26(3):311–21
63. Ratje AH, Loerke J, Mikolajka A, Brünner M, Hildebrand PW, et al. 2010. Head swivel on the ribosome facilitates translocation by means of intra-subunit tRNA hybrid sites. *Nature* 468(7324):713–16
64. Moazed D, Noller HF. 1989. Intermediate states in the movement of transfer RNA in the ribosome. *Nature* 342(6246):142–48
65. Frank J, Agrawal RK. 2000. A ratchet-like inter-subunit reorganization of the ribosome during translocation. *Nature* 406(6793):318–22
66. Valle M, Zavialov A, Sengupta J, Rawat U, Ehrenberg M, Frank J. 2003. Locking and unlocking of ribosomal motions. *Cell* 114(1):123–34
67. Brilot AF, Korostelev AA, Ermolenko DN, Grigorieff N. 2013. Structure of the ribosome with elongation factor G trapped in the pretranslocation state. *PNAS* 110(52):20994–99
68. Pulk A, Cate JHD. 2013. Control of ribosomal subunit rotation by elongation factor G. *Science*. 340(6140):1235970
69. Tourigny DS, Fernández IS, Kelley AC, Ramakrishnan V. 2013. Elongation factor G bound to the ribosome in an intermediate state of translocation. *Science* 340(6140):1235490
70. Sharma H, Adio S, Senyushkina T, Belardinelli R, Peske F, Rodnina MV. 2016. Kinetics of spontaneous and EF-G-accelerated rotation of ribosomal subunits. *Cell Rep.* 16:2187–96
71. Rodnina MV, Savelsbergh A, Katunin VI, Wintermeyer W. 1997. Hydrolysis of GTP by elongation factor G drives tRNA movement on the ribosome. *Nature* 385:37–41
72. Guo Z, Noller HF. 2012. Rotation of the head of the 30S ribosomal subunit during mRNA translocation. *PNAS* 109(50):20391–94
73. Zhou J, Lancaster L, Donohue JP, Noller HF. 2014. How the ribosome hands the A-site tRNA to the P site during EF-G-catalyzed translocation. *Science* 345(6201):1188–91

74. Adio S, Senyushkina T, Peske F, Fischer N, Wintermeyer W, Rodnina MV. 2015. Fluctuations between multiple EF-G-induced chimeric tRNA states during translocation on the ribosome. *Nat. Commun.* 6:7442
75. Chen C, Cui X, Beausang JF, Zhang H, Farrell I, et al. 2016. Elongation factor G initiates translocation through a power stroke. *PNAS* 113(27):7515–20
76. Bock L V, Blau C, Schröder GF, Davydov II, Fischer N, et al. 2013. Energy barriers and driving forces in tRNA translocation through the ribosome. *Nat. Struct. Mol. Biol.* 20(12):1390–96
77. Liu G, Song G, Zhang D, Zhang D, Li Z, et al. 2014. EF-G catalyzes tRNA translocation by disrupting interactions between decoding center and codon-anticodon duplex. *Nat. Struct. Mol. Biol.* 21(9):817–24
78. Marshall RA, Dorywalska M, Puglisi JD. 2008. Irreversible chemical steps control intersubunit dynamics during translation. *PNAS* 105(40):15364–69
79. Ermolenko DN, Majumdar ZK, Hickerson RP, Spiegel PC, Clegg RM, Noller HF. 2007. Observation of intersubunit movement of the ribosome in solution using FRET. *J. Mol. Biol.* 370(3):530–40
80. Gao Y, Selmer M, Dunham CM, Weixlbaumer A, Kelley AC, Ramakrishnan V. 2009. The structure of the ribosome with elongation factor G trapped in the posttranslocational state. *Science* 326:694–700
81. Chen C, Stevens B, Kaur J, Smilansky Z, Cooperman BS, Goldman YE. 2011. Allosteric vs. spontaneous exit-site (E-site) tRNA dissociation early in protein synthesis. *PNAS* 108(41):16980–85
82. Semenkov YP, Rodnina MV, Wintermeyer W. 1996. The "allosteric three-site model" of elongation cannot be confirmed in a well-defined ribosome system from Escherichia coli. *PNAS* 93(22):12183–88
83. Petropoulos AD, Green R. 2012. Further in vitro exploration fails to support the allosteric three-site model. *J. Biol. Chem.* 287(15):11642–48
84. Burkhardt N, Jünemann R, Spahn CM, Nierhaus KH. 1998. Ribosomal tRNA binding sites: three-site models of translation. *Crit. Rev. Biochem. Mol. Biol.* 33(2):95–149
85. Fei J, Bronson JE, Hofman JM, Srinivas RL, Wiggins CH, Gonzalez RL. 2009. Allosteric collaboration between elongation factor G and the ribosomal L1 stalk directs tRNA movements during translation. *PNAS* 106(37):15702–7
86. Triana-Alonso FJ, Chakraburtty K, Nierhaus KH. 1995. The elongation factor 3 unique in higher fungi and essential for protein biosynthesis is an E site factor. *J. Biol. Chem.* 270(35):20473–78
87. Pech M, Karim Z, Yamamoto H, Kitakawa M, Qin Y, Nierhaus KH. 2011. Elongation factor 4 (EF4/LepA) accelerates protein synthesis at increased Mg2+ concentrations. *PNAS* 108(8):3199–203
88. Machnicka MA, Milanowska K, Oglou OO, Purta E, Kurkowska M, et al. 2018. MODOMICS: a database of RNA modification pathways. 2017 update. *Nucleic Acids Res.* 46(D1):D303–7
89. He C. 2010. Grand challenge commentary: RNA epigenetics? *Nat. Chem. Biol.* 6(12):863–65
90. Saletore Y, Meyer K, Korlach J, Vilfan ID, Jaffrey S, Mason CE. 2012. The birth of the Epitranscriptome: deciphering the function of RNA modifications. *Genome Biol.* 13(10):175
91. Roundtree IA, Evans ME, Pan T, He C. 2017. Dynamic RNA modifications in gene expression regulation. *Cell* 169(7):1187–1200
92. Li X, Xiong X, Yi C. 2016. Epitranscriptome sequencing technologies: decoding RNA modifications. *Nat. Methods* 14(1):23–31
93. Lewis CJT, Pan T, Kalsotra A. 2017. RNA modifications and structures cooperate to guide RNA-protein interactions. *Nat. Rev. Mol. Cell Biol.* 18(3):202–10
94. Helm M, Motorin Y. 2017. Detecting RNA modifications in the epitranscriptome: predict and validate. *Nat. Rev. Genet.* 18(5):275–91
95. Dominissini D, Moshitch-Moshkovitz S, Schwartz S, Salmon-Divon M, Ungar L, et al. 2012. Topology of the human and mouse m6A RNA methylomes revealed by m6A-seq. *Nature* 485(7397):201–6
96. Meyer KD, Saletore Y, Zumbo P, Elemento O, Mason CE, Jaffrey SR. 2012. Comprehensive analysis of mRNA methylation reveals enrichment in 3′ UTRs and near stop codons. *Cell* 149(7):1635–46
97. Hoernes TP, Clementi N, Faserl K, Glasner H, Breuker K, et al. 2016. Nucleotide modifications within bacterial messenger RNAs regulate their translation and are able to rewire the genetic code. *Nucleic Acids Res.* 44(2):852–62
98. Roost C, Lynch SR, Batista PJ, Qu K, Chang HY, Kool ET. 2015. Structure and thermodynamics of N^6-methyladenosine in RNA: a spring-loaded base modification. *J. Am. Chem. Soc.* 137(5):2107–15

99. Choi J, Ieong K-W, Demirci H, Chen J, Petrov A, et al. 2016. N^6-methyladenosine in mRNA disrupts tRNA selection and translation-elongation dynamics. *Nat. Struct. Mol. Biol.* 23(2):110–15
100. Li X, Xiong X, Wang K, Wang L, Shu X, et al. 2016. Transcriptome-wide mapping reveals reversible and dynamic N^1-methyladenosine methylome. *Nat. Chem. Biol.* 12(5):311–16
101. Dominissini D, Nachtergaele S, Moshitch-Moshkovitz S, Peer E, Kol N, et al. 2016. The dynamic N^1-methyladenosine methylome in eukaryotic messenger RNA. *Nature* 530(7591):441–46
102. You C, Dai X, Wang Y. 2017. Position-dependent effects of regioisomeric methylated adenine and guanine ribonucleosides on translation. *Nucleic Acids Res.* 45(15):9059–67
103. Ge J, Yu YT. 2013. RNA pseudouridylation: new insights into an old modification. *Trends Biochem. Sci.* 38(4):210–18
104. King TH, Liu B, McCully RR, Fournier MJ. 2003. Ribosome structure and activity are altered in cells lacking snoRNPs that form pseudouridines in the peptidyl transferase center. *Mol. Cell.* 11(2):425–35
105. Fernández IS, Ng CL, Kelley AC, Wu G, Yu Y-T, Ramakrishnan V. 2013. Unusual base pairing during the decoding of a stop codon by the ribosome. *Nature* 500(7460):107–10
106. Karijolich J, Yu Y-T. 2011. Converting nonsense codons into sense codons by targeted pseudouridylation. *Nature* 474(7351):395–98
107. Schwartz S, Bernstein DA, Mumbach MR, Jovanovic M, Herbst RH, et al. 2014. Transcriptome-wide mapping reveals widespread dynamic-regulated pseudouridylation of ncRNA and mRNA. *Cell* 159(1):148–62
108. Carlile TM, Rojas-Duran MF, Zinshteyn B, Shin H, Bartoli KM, Gilbert WV. 2014. Pseudouridine profiling reveals regulated mRNA pseudouridylation in yeast and human cells. *Nature* 515(7525):143–46
109. Cummins LL, Owens SR, Risen LM, Lesnik EA, Freier SM, et al. 1995. Characterization of fully 2′-modified oligoribonucleotide hetero- and homoduplex hybridization and nuclease sensitivity. *Nucleic Acids Res.* 23(11):2019–24
110. Dai Q, Moshitch-Moshkovitz S, Han D, Kol N, Amariglio N, et al. 2017. Nm-seq maps 2′-*O*-methylation sites in human mRNA with base precision. *Nat. Methods* 14(7):695–98
111. Choi J, Indrisiunaite G, DeMirci H, Ieong K-W, Wang J, et al. 2018. 2′-*O*-methylation in mRNA disrupts tRNA decoding during translation elongation. *Nat. Struct. Mol. Biol.* 25:208–16
112. Novoa EM, Ribas de Pouplana L. 2012. Speeding with control: codon usage, tRNAs, and ribosomes. *Trends Genet.* 28(11):574–81
113. Richter JD, Coller J. 2015. Pausing on polyribosomes: make way for elongation in translational control. *Cell* 163(2):292–300
114. Presnyak V, Alhusaini N, Chen YH, Martin S, Morris N, et al. 2015. Codon optimality is a major determinant of mRNA stability. *Cell* 160(6):1111–24
115. Boël G, Letso R, Neely H, Price WN, Wong K-H, et al. 2016. Codon influence on protein expression in *E. coli* correlates with mRNA levels. *Nature* 529(7586):358–63
116. Gingold H, Tehler D, Christoffersen NR, Nielsen MM, Asmar F, et al. 2014. A dual program for translation regulation in cellular proliferation and differentiation. *Cell* 158(6):1281–92
117. Schmitt BM, Rudolph KLM, Karagianni P, Schmitt BM, Rudolph KLM, et al. 2014. High-resolution mapping of transcriptional dynamics across tissue development reveals a stable mRNA–tRNA interface. *Genome Res.* 24:1797–1807
118. Pavon-Eternod M, Gomes S, Geslain R, Dai Q, Rosner MR, Pan T. 2009. tRNA over-expression in breast cancer and functional consequences. *Nucleic Acids Res.* 37(21):7268–80
119. Goodarzi H, Nguyen HCB, Zhang S, Dill BD, Molina H, Tavazoie SF. 2016. Modulated expression of specific tRNAs drives gene expression and cancer progression. *Cell* 165(6):1416–27
120. Kirchner S, Ignatova Z. 2014. Emerging roles of tRNA in adaptive translation, signalling dynamics and disease. *Nat. Rev. Genet.* 16(2):98–112
121. Buhr F, Jha S, Thommen M, Mittelstaet J, Kutz F, et al. 2016. Synonymous codons direct cotranslational folding toward different protein conformations. *Mol. Cell.* 61(3):341–51
122. Pechmann S, Frydman J. 2012. Evolutionary conservation of codon optimality reveals hidden signatures of cotranslational folding. *Nat. Struct. Mol. Biol.* 20(2):237–43
123. Gamble CE, Brule CE, Dean KM, Fields S, Grayhack EJ. 2016. Adjacent codons act in concert to modulate translation efficiency in yeast. *Cell* 166(3):679–90

124. Yusupova GZ, Yusupov MM, Cate JHD, Noller HF. 2001. The path of messenger RNA through the ribosome. *Cell* 106(2):233–41
125. Jenner LB, Demeshkina N, Yusupova G, Yusupov M. 2010. Structural aspects of messenger RNA reading frame maintenance by the ribosome. *Nat. Struct. Mol. Biol.* 17(5):555–60
126. Chen C, Zhang H, Broitman SL, Reiche M, Farrell I, et al. 2013. Dynamics of translation by single ribosomes through mRNA secondary structures. *Nat. Struct. Mol. Biol.* 20(5):582–88
127. Liu T, Kaplan A, Alexander L, Yan S, Wen J-D, et al. 2014. Direct measurement of the mechanical work during translocation by the ribosome. *eLife* 3:e03406
128. Kontos H, Napthine S, Brierley I. 2001. Ribosomal pausing at a frameshifter RNA pseudoknot is sensitive to reading phase but shows little correlation with frameshift efficiency. *Mol. Cell. Biol.* 21(24):8657–70
129. Farabaugh PJ. 1996. Programmed translational frameshifting. *Annu. Rev. Genet.* 30:507–28
130. Mohammad F, Woolstenhulme CJ, Green R, Buskirk AR. 2016. Clarifying the translational pausing landscape in bacteria by ribosome profiling. *Cell Rep*. 14(4):686–94
131. Wohlgemuth I, Brenner S, Beringer M, Rodnina MV. 2008. Modulation of the rate of peptidyl transfer on the ribosome by the nature of substrates. *J. Biol. Chem.* 283(47):32229–35
132. Johansson M, Ieong K-W, Trobro S, Strazewski P, Åqvist J, et al. 2011. pH-sensitivity of the ribosomal peptidyl transfer reaction dependent on the identity of the A-site aminoacyl-tRNA. *PNAS* 108(1):79–84
133. Pavlov MY, Watts RE, Tan Z, Cornish VW, Ehrenberg M, Forster AC. 2009. Slow peptide bond formation by proline and other *N*-alkylamino acids in translation. *PNAS* 106(1):50–54
134. Melnikov S, Mailliot J, Rigger L, Neuner S, Shin B, et al. 2016. Molecular insights into protein synthesis with proline residues. *EMBO Rep*. 17(12):1776–84
135. Doerfel LK, Wohlgemuth I, Kothe C, Peske F, Urlaub H, Rodnina MV. 2013. EF-P is essential for rapid synthesis of proteins containing consecutive proline residues. *Science* 339(6115):85–88
136. Starosta AL, Lassak J, Peil L, Atkinson GC, Virumäe K, et al. 2014. Translational stalling at polyproline stretches is modulated by the sequence context upstream of the stall site. *Nucleic Acids Res*. 42(16):10711–19
137. Peil L, Starosta AL, Lassak J, Atkinson GC, Virumäe K, et al. 2013. Distinct XPPX sequence motifs induce ribosome stalling, which is rescued by the translation elongation factor EF-P. *PNAS* 110(38):15265–70
138. Gutierrez E, Shin BS, Woolstenhulme CJ, Kim JR, Saini P, et al. 2013. eIF5A promotes translation of polyproline motifs. *Mol. Cell.* 51(1):35–45
139. Ude S, Lassak J, Starosta AL, Kraxenberger T, Wilson DN, Jung K. 2013. Translation elongation factor EF-P alleviates ribosome stalling at polyproline stretches. *Science* 339:82–86
140. Doerfel LK, Wohlgemuth I, Kubyshkin V, Starosta AL, Wilson DN, et al. 2015. Entropic contribution of elongation factor P to proline positioning at the catalytic center of the ribosome. *J. Am. Chem. Soc.* 137(40):12997–13006
141. Woolstenhulme CJ, Guydosh NR, Green R, Buskirk AR. 2015. High-precision analysis of translational pausing by ribosome profiling in bacteria lacking EFP. *Cell Rep*. 11(1):13–21
142. Huter P, Arenz S, Bock LV, Graf M, Frister JO, et al. 2017. Structural basis for polyproline-mediated ribosome stalling and rescue by the translation elongation factor EF-P. *Mol. Cell.* 68(3):515–527.e6
143. Nam D, Choi E, Shin D, Lee EJ. 2016. $tRNA^{Pro}$-mediated downregulation of elongation factor P is required for *mgtCBR* expression during *Salmonella* infection. *Mol. Microbiol.* 102(2):221–32
144. Elgamal S, Katz A, Hersch SJ, Newsom D, White P, et al. 2014. EF-P dependent pauses integrate proximal and distal signals during translation. *PLOS Genet*. 10(8):e1004553
145. Nakatogawa H, Ito K. 2002. The ribosomal exit tunnel functions as a discriminating gate. *Cell* 108(5):629–36
146. Muto H, Nakatogawa H, Ito K. 2006. Genetically encoded but nonpolypeptide prolyl-tRNA functions in the A site for SecM-mediated ribosomal stall. *Mol. Cell.* 22(4):545–52
147. Bhushan S, Hoffmann T, Seidelt B, Frauenfeld J, Mielke T, et al. 2011. SecM-stalled ribosomes adopt an altered geometry at the peptidyl transferase center. *PLOS Biol*. 9(1):e1000581
148. Zhang J, Pan X, Yan K, Sun S, Gao N, Sui SF. 2015. Mechanisms of ribosome stalling by SecM at multiple elongation steps. *eLife* 4:4:e09684

149. Tsai A, Kornberg G, Johansson M, Chen J, Puglisi JD. 2014. The dynamics of SecM-induced translational stalling. *Cell Rep*. 7(5):1521–33
150. Navon SP, Kornberg G, Chen J, Schwartzman T, Tsai A, et al. 2016. Amino acid sequence repertoire of the bacterial proteome and the occurrence of untranslatable sequences. *PNAS* 113(26):7166–70
151. Tanner DR, Cariello DA, Woolstenhulme CJ, Broadbent MA, Buskirk AR. 2009. Genetic identification of nascent peptides that induce ribosome stalling. *J. Biol. Chem.* 284(50):34809–18
152. Vázquez-Laslop N, Mankin AS. 2014. Triggering peptide-dependent translation arrest by small molecules: ribosome stalling modulated by antibiotics. In *Regulatory Nascent Polypeptides*, ed. K Ito, S Chiba, pp. 165–86. Tokyo: Springer Jpn.
153. Arenz S, Meydan S, Starosta AL, Berninghausen O, Beckmann R, et al. 2014. Drug sensing by the ribosome induces translational arrest via active site perturbation. *Mol. Cell.* 56(3):446–52
154. Johansson M, Chen J, Tsai A, Kornberg G, Puglisi JD. 2014. Sequence-dependent elongation dynamics on macrolide-bound ribosomes. *Cell Rep*. 7(5):1534–46
155. Arenz S, Bock LV, Graf M, Innis CA, Beckmann R, et al. 2016. A combined cryo-EM and molecular dynamics approach reveals the mechanism of ErmBL-mediated translation arrest. *Nat. Commun*. 7:12026
156. Marks J, Kannan K, Roncase EJ, Klepacki D, Kefi A, et al. 2016. Context-specific inhibition of translation by ribosomal antibiotics targeting the peptidyl transferase center. *PNAS* 113(43):12150–55
157. Weisblum B. 1995. Erythromycin resistance by ribosome modification. *Antimicrob. Agents Chemother.* 39(3):577–85
158. Vazquez-Laslop N, Thum C, Mankin AS. 2008. Molecular mechanism of drug-dependent ribosome stalling. *Mol. Cell.* 30(2):190–202
159. Weisblum B. 1995. Insights into erythromycin action from studies of its activity as inducer of resistance. *Antimicrob. Agents Chemother.* 39(4):797–805
160. Lovett PS. 1996. Translation attenuation regulation of chloramphenicol resistance in bacteria—a review. *Gene* 179(1):157–62
161. Kannan K, Vázquez-Laslop N, Mankin AS. 2012. Selective protein synthesis by ribosomes with a drug-obstructed exit tunnel. *Cell* 151(3):508–20
162. Napthine S, Ling R, Finch LK, Jones JD, Bell S, et al. 2017. Protein-directed ribosomal frameshifting temporally regulates gene expression. *Nat. Commun.* 8:15582
163. Belew AT, Meskauskas A, Musalgaonkar S, Advani VM, Sulima SO, et al. 2014. Ribosomal frameshifting in the CCR5 mRNA is regulated by miRNAs and the NMD pathway. *Nature* 512(7514):265–69
164. Gupta P, Kannan K, Mankin AS, Vázquez-Laslop N. 2013. Regulation of gene expression by macrolide-induced ribosomal frameshifting. *Mol. Cell.* 52(5):629–42
165. Atkins JF, Elseviers D, Gorini L. 1972. Low activity of β-galactosidase in frameshift mutants of *Escherichia coli*. *PNAS* 69(5):1192–95
166. Jørgensen F, Kurland CG. 1990. Processivity errors of gene expression in *Escherichia coli*. *J. Mol. Biol.* 215(4):511–21
167. Parker J. 1989. Errors and alternatives in reading the universal genetic code. *Microbiol. Rev.* 53(3):273–98
168. Kramer EB, Farabaugh PJ. 2007. The frequency of translational misreading errors in *E. coli* is largely determined by tRNA competition. *RNA* 13(1):87–96
169. Sharma V, Prère MF, Canal I, Firth AE, Atkins JF, et al. 2014. Analysis of tetra- and hepta-nucleotides motifs promoting -1 ribosomal frameshifting in *Escherichia coli*. *Nucleic Acids Res.* 42(11):7210–25
170. Larsen B, Wills NM, Gesteland RF, Atkins JF. 1994. rRNA-mRNA base pairing stimulates a programmed −1 ribosomal frameshift. *J. Bacteriol.* 176(22):6842–51
171. Larsen B, Gesteland RF, Atkins JF. 1997. Structural probing and mutagenic analysis of the stem-loop required for *Escherichia coli dnaX* ribosomal frameshifting: programmed efficiency of 50%. *J. Mol. Biol.* 271(1):47–60
172. Kim H-K, Liu F, Fei J, Bustamante C, Gonzalez RL, Tinoco I. 2014. A frameshifting stimulatory stem loop destabilizes the hybrid state and impedes ribosomal translocation. *PNAS* 111(15):5538–43
173. Kim HK, Tinoco I. 2017. EF-G catalyzed translocation dynamics in the presence of ribosomal frameshifting stimulatory signals. *Nucleic Acids Res.* 45(5):2865–74
174. Koutmou KS, Schuller AP, Brunelle JL, Radhakrishnan A, Djuranovic S, Green R. 2015. Ribosomes slide on lysine-encoding homopolymeric A stretches. *eLife* 4:e05534

175. Arthur L, Pavlovic-Djuranovic S, Smith-Koutmou K, Green R, Szczesny P, Djuranovic S. 2015. Translational control by lysine-encoding A-rich sequences. *Sci. Adv.* 1(6):e1500154
176. Donly BC, Edgar CD, Adamski FM, Tate WP. 1990. Frameshift autoregulation in the gene for Escherichia coli release factor 2: Partly functional mutants result in frameshift enhancement. *Nucleic Acids Res.* 18(22):6517–22
177. Lobanov AV, Heaphy SM, Turanov AA, Gerashchenko MV, Pucciarelli S, et al. 2016. Position-dependent termination and widespread obligatory frameshifting in *Euplotes* translation. *Nat. Struct. Mol. Biol.* 24:585–97
178. Wang R, Xiong J, Wang W, Miao W, Liang A. 2016. High frequency of +1 programmed ribosomal frameshifting in *Euplotes octocarinatus*. *Sci. Rep.* 6:21139
179. Huang WM, Ao S, Casjens S, Orlandi R, Zeikus R, et al. 1988. A persistent untranslated sequence within bacteriophage T4 DNA topoisomerase gene 60. *Science* 239(4843):1005–12
180. Chen J, Coakley A, O'Connor M, Petrov A, O'Leary SE, et al. 2015. Coupling of mRNA structure rearrangement to ribosome movement during bypassing of non-coding regions. *Cell* 163(5):1267–80
181. Agirrezabala X, Samatova E, Klimova M, Zamora M, Gil-Carton D, et al. 2017. Ribosome rearrangements at the onset of translational bypassing. *Sci. Adv.* 3:e1700147
182. Samatova E, Konevega AL, Wills NM, Atkins JF, Rodnina MV. 2014. High-efficiency translational bypassing of non-coding nucleotides specified by mRNA structure and nascent peptide. *Nat. Commun.* 5:4459